Molecular and physiological characterization of arginine and proline catabolism in Arabidopsis

Dissertation

zur Erlangung des akademischen Grades eines

Doktors der Naturwissenschaften

an der

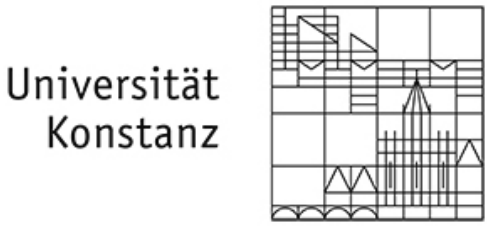

Mathematisch-naturwissenschaftliche Sektion

Fachbereich Biologie

Lehrstuhl für Physiologie und Biochemie der Pflanzen

vorgelegt von

Gudrun Winter

Tag der mündlichen Prüfung: 15.11.2013

1. Referent: Dr. Dietmar Funck

2. Referentin: Prof. Dr. Doris Rentsch

Table of Contents

Abstract

Plant productivity is frequently limited by the availability of nitrogen. Understanding the mechanisms of nitrogen acquisition, storage and recycling and their role in the metabolic and regulatory network of a plant cell is important to meet the demands of a growing human population for agricultural products. While the molecular mechanisms of nitrogen acquisition and assimilation are intensively studied, less is known about storage and recycling within the plant. Therefore, the focus of this study was on the catabolism of arginine in Arabidopsis and its function in transport, storage and recycling of nitrogen, in addition to its function as building block in protein synthesis or as precursor for polyamines.

Arginine biosynthesis and degradation is distributed over three cellular compartments - cytosol, plastids and mitochondria - which generates a need for specific transport systems for arginine as well as for synthesis and degradation intermediates In Arabidopsis, two intracellular arginine transporters, the basic amino acid carriers BAC1 and BAC2, were predicted to be mitochondrial proteins. I/We demonstrated the mitochondrial localization of the BAC proteins experimentally *in planta* and *in vivo*.

After import into mitochondria arginine is processed by the activities of two arginase isoenzymes (ARGAH1 and ARGAH2), ornithine-δ-aminotransferase (δOAT) and Δ^1-pyrroline-5-carboxylate dehydrogenase (P5CDH). Analysis of interaction characteristics of the arginine catabolising enzymes revealed homo- and hetero-oligomerisation of the arginase isoforms as well as homo-oligomerisation of P5CDH, pointing towards tissue specific arginase activity or pH dependent P5CDH activity. A specific polyclonal antibody against natively purified δOAT was raised, useful for pull down assays of native protein complexes from mitochondrial extracts and further investigations of enzyme complexes involving arginine degrading enzymes.

Investigating the physiological role of δOAT, it was found to contribute not significantly to very early seedling development, but in later stages of development. The retarded growth of δ*oat* mutants indicates an important role of δOAT activity for recycling of nitrogen from arginine in Arabidopsis and therefore an optimal plant internal nitrogen supply, directly associated with ideally plant productivity.

Zusammenfassung

Die Produktivität von Pflanzen ist häufig durch die Verfügbarkeit von Stickstoff begrenzt. Das Verständnis der Mechanismen von Stickstoffaufnahme, -speicherung und -wiederverwertung sowie deren Rolle im metabolischen und regulatorischen Netzwerk einer Pflanzenzelle ist von großer Bedeutung, um den Bedarf einer wachsenden Weltbevölkerung an landwirtschaftlichen Produkten befriedigen zu können. Während die molekularen Mechanismen der Stickstoffaufnahme und -assimilierung intensiv untersucht wurden, ist wenig über die Stickstoffspeicherung und -wiederverwertung in Pflanzen bekannt. Daher liegt der Fokus dieser Arbeit auf dem Katabolismus von Arginin und seiner Funktion im Transport, der Speicherung und Wiederverwertung von Stickstoff, neben der Rolle als Baustein in der Proteinsynthese oder als Vorstufe für Polyamine.

Die Synthese und der Abbau von Arginin sind über drei zelluläre Kompartimente verteilt - Cytosol, Plastiden und Mitochondrien - und erzeugen damit die Notwendigkeit spezifischer Transportsysteme für Arginin sowie für dessen Synthese- und Abbau- und Zwischenprodukte. Für zwei intrazelluläre Arginintransporter, die Carrier für basische Aminosäuren (BAC1 und BAC2), wurde eine Lokalistaion in Mitochondrien vorhergesagt. Die mitochondriale Lokalisation der BAC Proteine wurde im Rahmen dieser Arbeit experimentell *in planta* und *in vivo* bestätigt.

Nach dem mitochondrialen Import wird Arginin durch die Aktivitäten von zwei Arginase-Isoformen (ARGAH1 und ARGAH2), der Ornithin-δ-aminotransferase (δOAT) und der Δ^1-Pyrrolin-5-carboxylat Dehydrogenase (P5CDH) weiter prozessiert. Die Analyse der Interaktionscharakteristika der Arginin-abbauenden Enzyme zeigte eine Homo- und Hetero-Oligomerisierung der Arginase-Isoformen sowie die Homo-Oligomerisierung von P5CDH, was auf eine gewebespezifische Regulation der Arginase-Aktivität bzw. auf eine pH-abhängige Aktivität von P5CDH hinweist. Gegen nativ aufgereinigtes Protein der δOAT wurde ein spezifischer polyklonaler Antikörper hergestellt, einsetzbar für Immunopräzipitationen von nativen Proteinkomplexen aus mitochondrialen Extrakten und weiteren Untersuchungen, um die Existenz von Enzymkomplexen unter Beteiligung von Arginin-abbauenden Enzymen zu analysieren.

Untersuchungen zur physiologischen Rolle von δOAT zeigten keine signifikante Beteiligung von δOAT in der frühen Keimlingsentwicklung, jedoch in späteren Phasen der Pflanzenentwicklung. Das verzögerte Wachstum der δ*oat* Mutanten spricht für eine wichtige Rolle der Aktivität von δOAT in der Wiederverwertung von, in Arginin gespeichertem, Stickstoff in Arabidopsis und damit für eine Rolle in der optimalen Pflanzen-internen Stickstoffversorgung, welche wiederum direkt mit der Produktivität von Pflanzen verbunden ist.

1. Introduction

As the most prominent and most expensive fertiliser component, nitrogen (N) is an essential input in agricultural production because it is often limiting for plant growth, development and fruit production. In 2009 the total estimated application of fertilizers in the EU averaged 76 kilograms of nutrients (total sum of N, phosphorus (P) and potassium (K)) per hectare of utilized agriculture area. Nitrogen accounted for the major part (78 %) of the fertilizers, with an estimated application of 59 kg/ha on average (Figure 1, Eurostat (2011)).

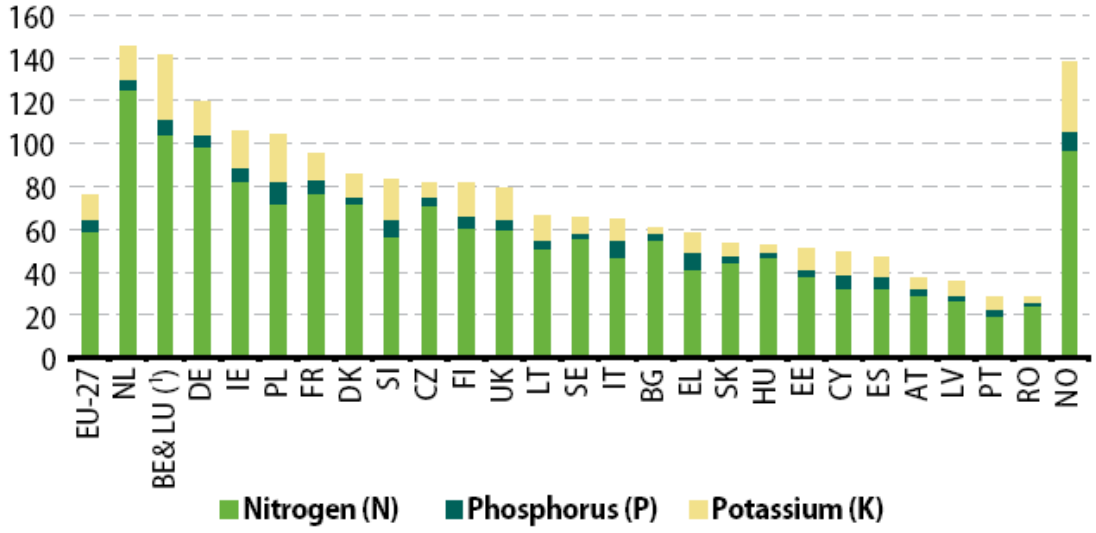

Figure 1: Estimated consumption of manufactured fertilizers, 2009 (Kilograms of nutrient per hectare of utilized agricultural area)

Nitrogen is the most prominent fertilizer component in the European Union. EU-27: Average of the 27 EU member states; NL: Netherlands; BE&LU(1): Belgium-Luxembourg Economic Union; DE: Germany; IE: Ireland; PL: Poland; FR: France; DK: Denmark; SI: Slovenia; CZ: Czech Republic; FI: Finland; UK: United Kingdom; LT: Lithuania; SE: Sweden; IT: Italy; BG: Bulgaria; EL: Greece; SK: Slovak Republic; HU: Hungary; EE: Estonia; CY: Cyprus; ES: Spain; AT: Austria; LV: Latvia; PT: Portugal; RO: Romania; NO: Norway; Source: Agriculture and fishery statistics, Main results - 2009–10

Nitrogen uptake through dedicated transport systems in the roots of plants is described in several studies (Yuan *et al.*, 2007; Krouk *et al.*, 2010; Arsova *et al.*, 2012). Nitrogen is mainly supplied as nitrate and ammonium salts (Arsova *et al.*, 2012) or in form of urea (Witte, 2011). Also amino acids are assimilated by plants and function as nitrogen source (Forsum *et al.*, 2008; Svennerstam *et al.*, 2008). A

series of enzymes processes the assimilation of inorganic nitrogen into the organic molecules. Nitrate is reduced to nitrite by nitrate reductase. The following plastid-localized nitrite reductase produces ammonium (Arsova *et al.*, 2012). The nitrogen comprised in urea is only accessible for assimilation after hydrolysis to ammonia and carbon dioxide. Its matter of discussion if plants mainly take up ammonium and nitrate generated by microbial conversion of urea in the soil or if plants are able to take up urea directly by urea transporters and generate ammonium by internal hydrolysis (Witte, 2011). The use of ammonium for incorporation into amino acids is advantageous for plants with respect to costs for energy and reducing power and is processed by the combined activity of glutamine synthase (GS) and glutamate synthase (GOGAT), using α-ketoglutarate to generate glutamate (Llacer *et al.*, 2008). Subsequently, glutamate provides amino groups for the synthesis of amino acids and other nitrogen containing compounds.

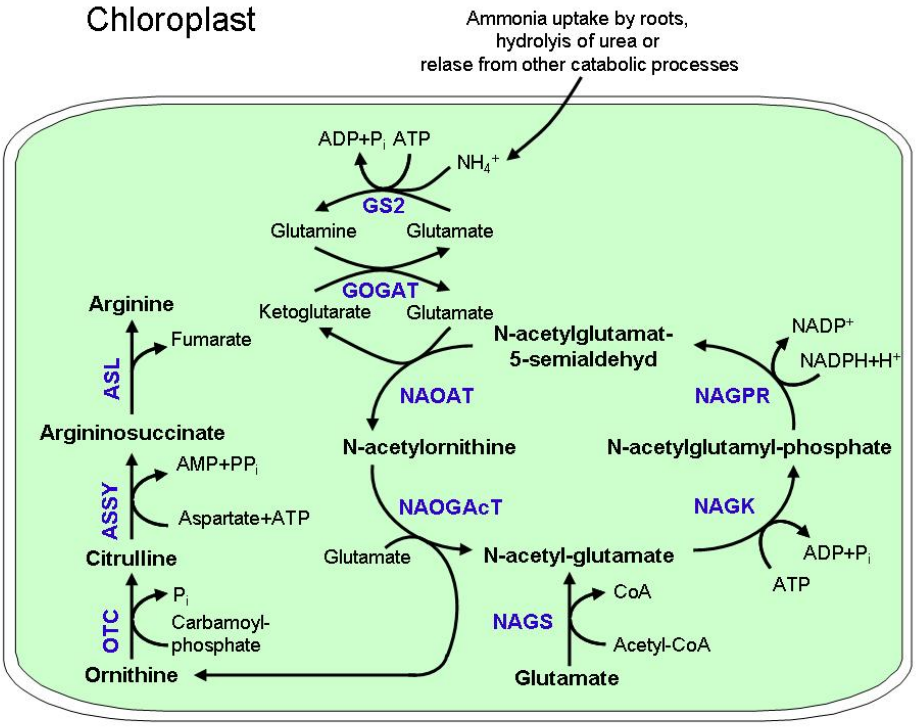

Figure 2: Ammonium assimilation by the GS2/GOGAT-system and its connection to arginine synthesis in plastids

GS2: Glutamine synthase 2; GOGAT: Glutamate synthase; NAGS: N-acteyl-glutamate synthase; NAGK: N-acetyl-glutamate kinase; NAGPR: N-acetyl-glutamyl-5-P reductase; NAOAT: N-acetyl-ornithine aminotransferase; NAOGAcT: N-acetyl-ornithine-glutamate acteyltransferase; OTC: Ornithine transcarbamylase; ASSY: Argininosuccinate synthase; ASL: Argininosuccinate lyase, CoA: Coenzyme A

In contrast to the cytosolic GS1, the GS2/GOGAT-system is located in the plastid (Masclaux-Daubresse *et al.*, 2006; Arsova *et al.*, 2012). Sharing the same subcellular localization it can directly be coupled to arginine biosynthesis by the activity of N-acetyl-ornithine transferase (NAOAT) (Figure 2). Due to the high nitrogen to carbon ratio, arginine is a major storage and transport form for organic nitrogen in plants and arginine metabolism, especially its catabolism plays a key role in nitrogen distribution and recycling (Brauc *et al.*, 2012).

1.1. Arginine biosynthesis

The biosynthetic pathway of arginine can be divided in two processes. First ornithine is synthesized from glutamate in the 'cyclic pathway', followed by the synthesis of arginine from ornithine (Slocum, 2005) (Figure 2 and Figure 3).

1.1.1. Cyclic and linear pathways for ornithine synthesis

Ornithine is synthesized from glutamate *via* several acetylated intermediates (Figure 2). This was first demonstrated in plants by Dougall and Fulton (1967). Later investigations revealed that the enzymes catalyzing the first four steps are conserved in plants (Shargool *et al.*, 1988) and other organisms (Cunin *et al.*, 1986; Davis, 1986). In non-enteric bacteria (Cunin *et al.*, 1986), fungi (Davis, 1986) and plants (Shargool *et al.*, 1988; Slocum, 2005) the enzyme N-acetylornithine:N-acetylglutamate acetyltransferase (NAOGAcT) plays a key role in transferring an acetyl group from acetylornithine to glutamate, thus conserving the acetyl group with the formation of acetyl glutamate and ornithine. The 'cyclic pathway' for ornithine synthesis is completed by this step. To start this cycle, N-acetylglutamate synthase uses Acetyl-coenzyme A (Acetyl-CoA) to transfer an acetyl moiety to glutamate (Slocum, 2005).

E. coli is able to synthesise ornithine in a linear pathway by the activity of N-acetylornithine deacetylase (NAOD), which converts N-acetylornithine and H_2O to ornithine and acetate (Vogel and Bonner, 1956). Plants are presumably unable to use this pathway, since NAOD activity has not been demonstrated in plants so far (Slocum, 2005).

Glutamate is a precursor for both proline and ornithine biosynthesis in plants and other organisms (Morris *et al.*, 1969; Cunin *et al.*, 1986; Davis, 1986; Caldovic and Tuchman, 2003). After acetylation of glutamate, the N-acetylglutamate semialdehyde (NAcGSA) intermediate is incapable of undergoing cyclisation. This feature commits it to ornithine synthesis. In contrast, the corresponding non-acetylated glutamate semialdehyde (GSA) in proline biosynthesis spontaneously forms pyrroline-5-carboxylate (P5C) by cyclisation (Slocum, 2005).

1.1.2. Arginine synthesis from ornithine

Arginine is synthesized from ornithine by the enzymes of the linear 'arginine pathway' (Micallef and Shelp, 1989; Slocum, 2005). Ornithine transcarbamoylase (OTC) catalyzes carbamoylation of the δ-amino group of ornithine, forming citrulline. Citrulline is further metabolized *via* argininosuccinate synthase (ASSY) and argininosuccinate lyase (ASL) activities (Slocum, 2005) generating the final product arginine (Figure 3).

1.2. Arginine utilisation and transport

After biosynthesis, arginine can be used for protein synthesis directly in plastids or, after export, in the cytosol and mitochondria. Besides being a building block of proteins, arginine is a precursor for the synthesis of polyamines (putrescine, spermidine and spermine) (Bagni and Tassoni, 2001; Illingworth *et al.*, 2003). Polyamines are essential for growth of plants and are involved in diverse physiological responses, including cell division, tuber formation, root initiation, embryogenesis, flower development and fruit ripening (Buchanan *et al.*, 2006). For starting polyamine biosynthesis in Arabidopsis arginine is converted by the plastid localized arginine decarboxylase (ACD) to agmatine (Borrell *et al.*, 1995), followed by enzymes of polyamine synthesis with so far unknown localization (Figure 3). In contrast to other plants Arabidopsis is not able to synthesise putrescine directly by decarboxylation of ornithine, since Arabidopsis lacks an ornithine decarboxylase (ODC) gene (Hanfrey *et al.*, 2001).

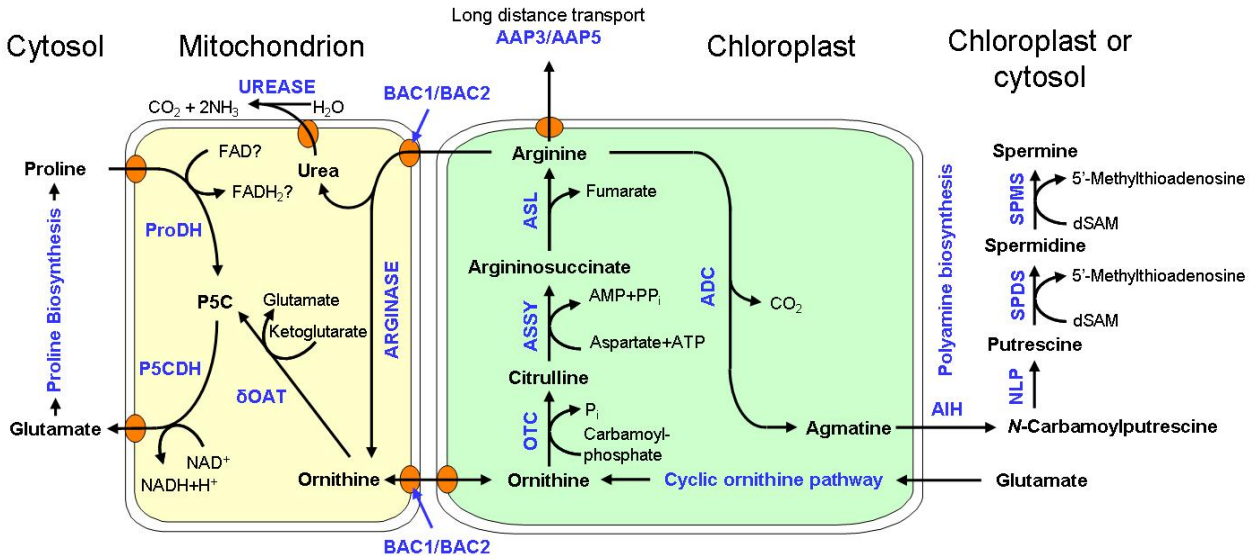

Figure 3: Metabolism of arginine and its utilization in Arabidopsis

OTC: Ornithine transcarbamylase; ASSY: Argininosuccinate synthase; ASL: Argininosuccinate lyase; BAC1/BAC2: Basic amino acid transporter 1/2; δOAT: Ornithine-δ-aminotransferase; ProDH: Proline dehydrogenase; P5CDH: P5C dehydrogenase; P5C: pyrroline-5-carboxylate, ADC: Arginine decarboxylase; AIH: Agmatine iminohydrolase (agmatine deiminase) (Janowitz *et al.*, 2003); NLP: *N*-carbamoylputrescine amidase (Piotrowski *et al.*, 2003), SPDS: Spermidine synthase (Hanzawa *et al.*, 2002); SPMS: Spermine synthase, dSAM: Decarboxylated *S*-Adenosyl-L-methionine, AAP3/AAP5: Amino acid permease 3/5

In addition to being an amino acid in protein synthesis or precursor for polyamines, arginine is essential for many cellular and developmental processes. Transport or storage of nitrogen is the most important function of arginine. 40-50 % of the total nitrogen reserve in seed protein in different plant species is arginine (VanEtten *et al.*, 1963; King and Gifford, 1997). 50 % of the nitrogen in free amino acids is in the arginine pool in developing embryos of soybean (Micallef and Shelp, 1989) and pea (de Ruiter and Kolloffel, 1983).

Long distance transport to nitrogen storing organs or seeds occurs probably in the phloem and xylem and is presumably mediated by amino acid permeases (AAP3 and AAP5), which are loading and unloading the vascular tissue (Fischer *et al.*, 1995; Fischer *et al.*, 2002; Okumoto *et al.*, 2004; Svennerstam *et al.*, 2008). AAP5 transports arginine and lysine with high affinity (Svennerstam *et al.*, 2008) and is mainly discussed to be responsible for uptake of basic amino acids by roots. However, being expressed throughout the whole plant (Fischer *et al.*, 1995; Fischer

et al., 2002; Svennerstam *et al.*, 2008) it is conceivable, that AAP5 has also a transport function for arginine within plants. AAP3 displays high affinity for basic amino acids (Fischer *et al.*, 2002) and was shown to be expressed in the stele, mediating phloem loading of amino acids (Okumoto *et al.*, 2004) and therefore probably responsible for distribution of arginine in the plant, too.

Distribution of arginine biosynthesis and degradation over the three cellular compartments cytosol, plastids and mitochondria generates a need for specific transport systems for arginine as well as for synthesis and degradation intermediates. Transport proteins, like the basic amino acid transporters, are essential for the import of arginine into mitochondria for degradation and therefore for the movement of metabolites between the cytosol and the mitochondrial matrix.

1.2.1. Basic amino acid transporters

Protein transporters are essential for an efficient transport of polymeric molecules between the cytosol and the mitochondrial matrix. The prevalent group of carrier proteins in mitochondria is the mitochondrial carrier family (MCF) with 58 putative members (Picault *et al.*, 2004; Haferkamp and Schmitz-Esser, 2012) in Arabidopsis. Two members of the MCF were identified as basic amino acid transporters (BAC1 and BAC2) which mediate the transport of arginine, ornithine and lysine with decreasing affinity and were postulated to be localized in the mitochondrial inner membrane (Hoyos *et al.*, 2003; Palmieri *et al.*, 2006).

BAC1 and BAC2 were identified as basic amino acid transporters by complementation of the yeast mutant *arg11*. This mutant is defective in mitochondrial ornithine/arginine transport due to a loss-of-function mutation in the ORT1 carrier (Catoni *et al.*, 2003; Hoyos *et al.*, 2003; Palmieri *et al.*, 2006). ORT1 is an ornithine, arginine and lysine antiporter, important for ornithine export from mitochondria, an essential step for arginine biosynthesis in *Saccharomyces cerevisiae* (Palmieri *et al.*, 1997; Palmieri *et al.*, 2006).

The *BAC1* gene (At2g33820) (Hoyos *et al.*, 2003) encodes a 936-bp transcript. The *BAC2* gene (At1g79900) (Catoni *et al.*, 2003; Hoyos *et al.*, 2003) produces a longer 1455-bp transcript. Both predicted amino acid sequences show characteristic

features of MCF proteins (Picault *et al.*, 2004; Haferkamp and Schmitz-Esser, 2012). BAC1, BAC2 and BOU (Lawand *et al.*, 2002) form a sub-group of proteins distinct from other Arabidopsis mitochondrial carriers regarding sequences and function (Catoni *et al.*, 2003; Hoyos *et al.*, 2003; Picault *et al.*, 2004; Toka *et al.*, 2010). The complementation of the *arg11* mutant suggests that BAC1 and BAC2 are mitochondrial proteins, too. This study shows mitochondrial localization for BAC2 and for the first time also for BAC1.

1.3. Arginine catabolism

After the import of arginine by BAC1 and BAC2 into mitochondria, arginine catabolism starts with degradation of arginine by arginase to ornithine followed by the activity of ornithine δ-aminotransferase (δOAT) processing ornithine further to Δ^1-pyrroline-5-carboxylate (P5C). P5C is subsequently converted to glutamate by P5C dehydrogenase (P5CDH). Glutamate can be recycled or be degraded to α-ketoglutarate, ammonium and NADH by glutamate dehydrogenase (GDH). NADH is used as energy equivalent for the respiratory chain and ammonium as well as α-ketoglutarate can be recycled in the GS/GOGAT system (Buchanan *et al.*, 2006).

1.3.1. Arginase

For recycling of nitrogen from arginine the amino acid has to be imported into mitochondria where it is catabolised to ornithine and urea by arginase activity (L-arginine ureahydrolase or amidinohydrolyase) (Goldraij and Polacco, 2000; Todd *et al.*, 2001). Zonia *et al.* (1995) showed a 10-fold increase in total arginase activity from 0 to 6 days after germination (DAG) in Arabidopsis accompanied by increases in free arginine and urea levels. The amino acid sequences of the two Arabidopsis arginase structural genes, ARGAH1 (At4g08900) (Krumpelman *et al.*, 1995) and ARGAH2 (At4g08870) (Flores *et al.*, 2008) show 86 % sequence identity including the predicted mitochondrial transit peptide. The N-terminal amino acids of the predicted mitochondrial transit peptides contain most differences (only 39 % sequence identity), while the C-terminal amino acids belonging to the predicted

protein after N-terminal processing are 91 % identical (Flores *et al.*, 2008). GFP-fusion proteins showed ARGAH1 and ARGAH2 to be both mitochondrial proteins (Palmieri *et al.*, 2006; Flores *et al.*, 2008).

Arginase is a binuclear manganese metalloenzyme that catalyzes the hydrolysis of L-arginine to L-ornithine and urea (Dowling *et al.*, 2008). Crystal structures of arginases revealed a homo-trimeric quartenary structure for rat arginase 1 (Kanyo *et al.*, 1996) and human arginase 1 (Di Costanzo *et al.*, 2007) and 2 (Cama *et al.*, 2003), as well as homo-hexameric arginases from *Bacillus caldovelox* (Bewley et al., 1999) and *Thermus thermophilus* (Dowling *et al.*, 2008). Arginases have been purified and characterized from different plant species such as soybean (Kang and Cho, 1990), iris bulbs (Boutin, 1982), peanut seedlings (Desai, 1983), oakmoss (Martin-Falquina and Legaz, 1984) and ginseng (Hwang *et al.*, 2001), showing variable sizes of monomers and oligomers. For arginase purified from Catjang (*Vigna unguiculata*) a native molecular weight of 210 kDa was estimated, while the monomer had an apparent molecular weight of 52 kDa (Dabir *et al.*, 2005). This supports a tetrameric structure of arginase from Catjang. In contrast, arginase purified from ginseng was estimated to be decameric (Hwang *et al.*, 2001). So far, nothing is known about the oligomerisation or structure of arginase from Arabidopsis.

Arginine catabolism by arginase releases urea (Goldraij and Polacco, 2000) and regenerates ornithine, which can be transported back to the plastids for biosynthesis of arginine *via* the arginine pathway again (Figure 3). However, cycling between ornithine and arginine is unlikely to occur in a single cell or tissue in plants, as it would constitute a waste of energy and assimilated nitrogen. More likely is a further degradation of ornithine by δOAT, which catalyzes the conversion of ornithine to P5C/GSA and metabolically links proline and arginine catabolism (Roosens *et al.*, 1998; Funck *et al.*, 2008).

1.3.2. Ornithine δ-aminotransferase

δOAT is the second enzyme of arginine catabolism and converts ornithine to GSA and glutamate by transferring the δ-amino group of ornithine to α-ketoglutarate. GSA spontaneously forms the cyclic P5C, which is a common intermediate of

proline and arginine degradation. The equilibrium of the δOAT reaction has been found far on the GSA/glutamate side (Adams and Frank, 1980).

A contribution of δOAT to stress induced proline accumulation, which would require an unknown exit route of mitochondrial P5C to the cytosol, where P5C reductase (P5CR) is localized, is controversially discussed (Stranska *et al.*, 2008). Roosens *et al.* (1998) hypothesized that δOAT plays an important role in proline accumulation during osmotic stress in plants, because of increased free proline content, δOAT activity and δOAT mRNA in young Arabidopsis plantlets under salt-stress conditions. This hypothesis is consistent with transgenic *Nicotiana plumbaginifolia* plants overexpressing Arabidopsis δOAT, synthesizing more proline than the control plants and showing a higher biomass and a higher germination rate under osmotic stress conditions (Roosens *et al.*, 2002). Targeting of δOAT to mitochondria was the first evidence which strongly suggested that P5C generated by δOAT activity enters the degradation pathway of proline rather than its biosynthesis (Funck *et al.*, 2008) (Figure 4). Proline production *via* ProDH is energetically unfavourable and due to the chemical instability of GSA/P5C (Williams and Frank, 1975) and its toxicity when accumulating (Deuschle *et al.*, 2004), export from mitochondria to the cytosol and thus contribution to proline synthesis is unlikely but can not be fully excluded (Funck *et al.*, 2008). In addition *δoat* mutants did not show altered proline levels and displayed the same salt stress responses as wild type plants, which suggests that δOAT does not contribute to stress-induced proline accumulation (Funck *et al.*, 2008).

P5C produced by δOAT inside mitochondria is most probably further converted to glutamate by mitochondrial P5CDH (Figure 4) consistent with the proven mitochondrial localization of δOAT and P5CDH (Deuschle *et al.*, 2001; Funck *et al.*, 2008). Due to the mentioned chemical instability and toxicity of GSA/P5C the formation of a reversible enzyme complex of δOAT and P5CDH seems likely, exchanging P5C without releasing it to the mitochondrial matrix (Elthon and Stewart, 1982; Funck *et al.*, 2008) and yielding the final product, one molecule of glutamate which can be transported out of the mitochondria to re-enter proline synthesis or other metabolic processes.

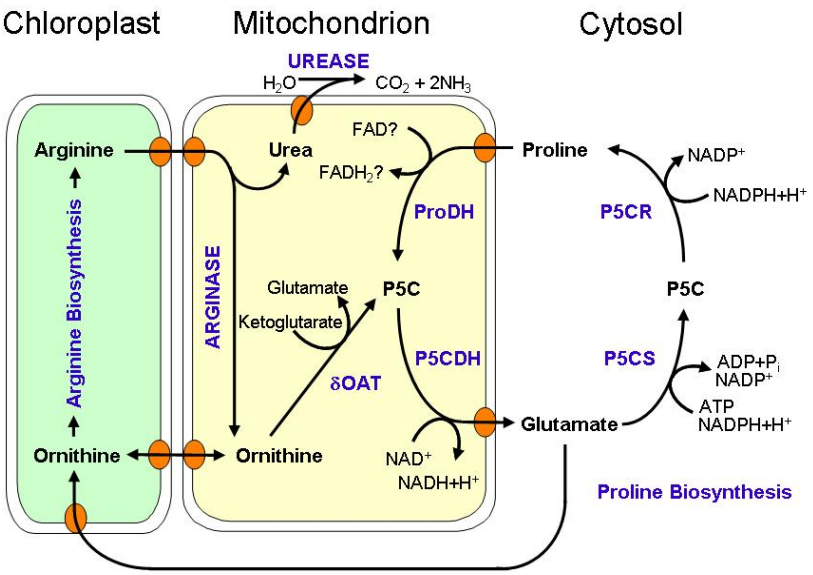

Figure 4: Arginine catabolism and proline metabolism in Arabidopsis

δOAT: Ornithine δ-aminotransferase; ProDH: Proline dehydrogenase; P5CDH: P5C dehydrogenase; P5C: pyrroline-5-carboxylate, P5CS: P5C synthase, P5CR: P5C reductase

Physiological experiments with Arabidopsis *δoat* mutants have shown that they were unable to use arginine or ornithine as sole source of nitrogen, demonstrating that degradation of ornithine depends on δOAT activity (Funck *et al.*, 2008). When growing on medium lacking mineral nitrogen but supplemented with sucrose, low amounts of glutamine (to enable growth) and arginine or ornithine (as additional organic nitrogen source) δ*oat* mutants showed accumulation of ornithine and urea under these nutritional conditions. In addition, stress-induced proline accumulation was not affected by the mutation of δOAT. These results provided again strong evidence against a shortcut from arginine to proline that bypasses glutamate and cytosolic P5CS activity and suggest an important role of δOAT for arginine catabolism and nitrogen recycling, but not for the stress-induced proline accumulation (Funck *et al.*, 2008). It is conceivable, that ornithine can be converted to proline only *via* glutamate under normal physiological conditions (Figure 4).

Polyamines were found to be non-competitive inhibitors for pea δOAT (Stranska *et al.*, 2010). It seems that increased polyamine concentrations can significantly reduce the activity of pea δOAT *in vivo* and Stranska *et al.* (2010) hypothesized this would result in slowing down arginine catabolism. Since polyamines are involved in diverse physiological responses it is advantageous for plants slowing down

arginine catabolism in favour of polyamine synthesis (Figure 3) if necessary. This is probably more effective in pea, since a gene encoding ornithine decarboxylase (ODC) exists in the genome of *Pisum sativum*. ODC converts ornithine directly to putrescine and represents an alternative metabolic pathway for polyamine biosynthesis in contrast to Arabidopsis, which lacks an ODC (Hanfrey *et al.*, 2001) and need to synthesize all polyamines starting from arginine *via* ADC followed by the enzymes of polyamine synthesis (Figure 3).

Regulation of arginine catabolism in Arabidopsis is still matter of investigation, but δ*oat* mutants, where mitochondrial arginine catabolism is blocked, displayed increased contents in ornithine, indicating that arginase is not efficiently down-regulated by ornithine (Funck *et al.*, 2008). In contrast, δ*oat* mutants showed decreased levels of arginine, suggesting that arginine biosynthesis is probably subject of feedback inhibition through localized increase of arginine or ornithine concentrations (Funck *et al.*, 2008).

1.4. Protein oligomerisation and multi-enzyme complexes

Arginine metabolism is highly compartmentalised as pathways are separated, biosynthesis to plastids and catabolism to mitochondria. Compartmentation is essential for metabolic regulation in eukaryotic cells. Many metabolic pathways are highly compartmentalised, for example, between different subcellular organelles, which concentrates enzymes and metabolites and also separates them, as a means of controlling reactions, to avoid futile cycling or undesired cross-talk between pathways with common intermediates (Bowsher and Tobin, 2001). For understanding of a eukaryotic cell network, it is necessary to know how metabolism and other processes are compartmented within the cell and also how they are all linked and controlled. In comparison to animal cells, plant cells contain additional compartments - plastids, cell walls and vacuoles - and feature a greater diversity of metabolic pathways, making investigations on plant metabolic network particularly challenging (Lunn, 2007).

Metabolism in every compartment depends, to some extent, on other parts of the cell for supplies of energy (ATP) or metabolic precursors. Additionally, all compartments rely on nuclear gene expression and cytosolic translation, which

provide most of their enzymes and other proteins. Each enzyme in a particular pathway is fine-tuned by the regulatory network of the cell. For a functional control of enzymes, protein homo- or hetero-oligomerisation plays an important role.

Oligomeric proteins comprise two or more associating polypeptide chains. At least 35 % of all proteins in a cell were suggested to form oligomers (Goodsell and Olson, 2000). The majority of oligomeric proteins are homo-oligomeric (Goodsell and Olson, 2000) and it has been estimated that the average oligomeric state is tetrameric (Goodsell, 1991). Higher-order oligomers are less prevalent (Jones and Thornton, 1996; Goodsell and Olson, 2000) and a relatively small fraction of oligomeric structures have oddnumbered stoichiometries (Ali and Imperiali, 2005).

Several functional advantages are conferred by oligomerisation:

- Monomer and oligomer can differ in activity. Regulating the conditions of oligomerisation may result in additional regulatory flexibility (Ali and Imperiali, 2005).

- A large protein composed of multiple, short, subunits is more likely to be synthesized without errors than a single chain protein of comparable size (Goodsell and Olson, 1993; Ali and Imperiali, 2005).

- Function could be supported by more complex scaffolds, for example by the introduction of a new active site at the interface between subunits (Goodsell and Olson, 1993; Ali and Imperiali, 2005).

- Larger proteins are more resistant to degradation and denaturation, as demonstrated by thermophilic organisms increasing the oligomerisation state as one of the protein stabilization strategies (Walden *et al.*, 2001).

Cellular metabolism involves not only compartmentation, to specify the spatial distribution of pathways, or oligomerisation, for regulation and stability of proteins, but also multi-enzyme complexes. Multi-enzyme complexes are similar to hetero-oligomeric proteins, because different polypeptide chains are assembled to one complex, but multi-enzyme complexes may contain two or more homo- or hetero-oligomeric enzymes resulting in bigger and more complex structures. Cooperating enzymes assemble into complexes, often associated with structural elements within the cell (Ovadi and Srere, 2000; Srere, 2000). Therefore metabolic

processes have the ability to 'channel' intermediates between two or more active sites without releasing them into the aqueous compartments of the cell, where other enzymes may get access to the intermediate (Mathews, 1993; Spivey and Ovadi, 1999). Multi-enzyme complexes and therefore metabolic channelling are advantageous as a means to cope with high local substrate concentrations, regulate competition between pathways for common metabolites or the activities of pathways with common enzymes or intermediates and separate reactive or toxic intermediates (Winkel, 2004).

Most of the mentioned advantages of multi-enzyme complexes apply to the potential reversible enzyme complex of δOAT and P5CDH inside mitochondria during arginine catabolism, which would 'channel' P5C without releasing it to the mitochondrial matrix (Elthon and Stewart, 1982; Funck *et al.*, 2008). Investigating this potential multi-enzyme complex was one of the aims of this work.

1.5. Aims of this work

Determination of the exact role of a specific enzyme in the metabolic and regulatory network of a plant cell requires careful and thorough gene for gene analysis. The knowledge about arginine and its catabolism is still fragmentary on the level of the subcellular localization of the intracellular arginine transporters as well as characteristics of the degradation enzymes arginase and δOAT.

With the start of this study the localization of both Arabidopsis BAC transporters was only inferred from their affiliation to the MCF and from heterologous expression in yeast. One aim of this work was to determine the localization of the BAC proteins *in planta* and *in vivo* by analysis of transgenic plants expressing BAC-GFP fusion proteins. Verified by confocal laser scanning microscopy this study clearly demonstrates that both transporters are targeted exclusively to mitochondria.

Biochemical studies on intact mitochondria had suggested the formation of multi-enzyme complexes between particular enzymes of arginine catabolism (Elthon and Stewart, 1982). Substrate channelling in arginine catabolism can be decisive for the fate of the degradation products and therefore the possible connections between

arginine and proline metabolism. Investigating the formation of reversible enzyme complexes of δOAT and P5CDH, exchanging P5C without releasing it to the mitochondrial matrix was one aim of this work. Putative enzyme interactions at the molecular level were analysed applying yeast two hybrid (Y2H) interaction assays, direct interaction analyses of recombinant proteins and *in vivo* studies with BIFC. Addressing the question of cell and tissue dependent regulation of enzyme activities in arginine catabolism oligomerisation characteristics of arginase were investigated and provide evidence for so far unknown homo- and heterooligomerisation of Arabidopsis arginase isoenzymes.

Besides interaction characteristics and involvement in the metabolic network of the plant cell, the physiological role of arginine breakdown and especially of δOAT in Arabidopsis plants is of great interest. The contribution of δOAT activity in very early seedling development, especially in seed production and expansion growth of seedlings or at later stages of development was another aim of this work and revealed an important role of δOAT activity for recycling of nitrogen from arginine in Arabidopsis.

2. Results and Discussion

2.1. BAC1 and BAC2 are exclusively mitochondrial proteins

The two basic amino acid carriers BAC1 and BAC2 were assumed to be localized in mitochondria as they belong to the MCF protein family and were able to complement a mitochondrial transporter mutant in yeast. GFP-fusion proteins were used for stable and transient expression of GFP-tagged BAC1 and BAC2 to determine the subcellular localization of these two proteins *in planta*.

While the majority of MCF proteins are localized in the inner mitochondrial membrane, other family members were detected in plastids, peroxisomes, the plasma membrane and the ER (Haferkamp and Schmitz-Esser, 2012). Therefore, it is important to analyze the subcellular localization of MCF proteins in order to correctly identify their physiological function. For this study Arabidopsis wild type plants were stably transformed with fusion constructs of BAC1-GFP and BAC2-GFP coding sequences under the control of the 35S cauliflower mosaic virus promoter. Epifluorescence microscopy of leaf epidermal cells (Figure 5) and confocal microscopy of protoplasts (Figure 6 and Figure 7) from transgenic plants showed GFP fluorescence in mitochondria, confirmed by co-localization with the mitochondria-specific fluorescent dye MitoTracker orange. Three independent transformants of BAC1-GFP and BAC2-GFP respectively showed the same fluorescent pattern.

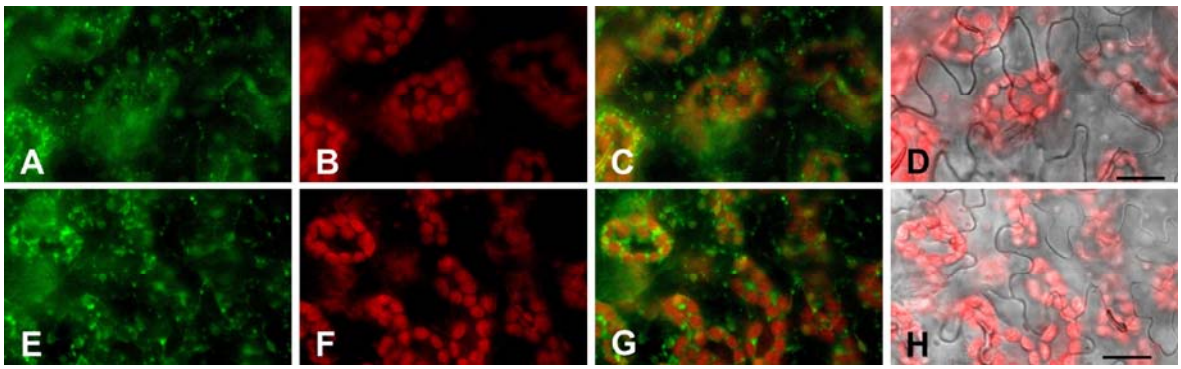

Figure 5: BAC-GFP fluorescence *in vivo* is consistent with mitochondrial localization

False coloured epifluorescence images of leaf epidermis cells and underlying spongy mesophyll cells of Arabidopsis plants stably expressing BAC1-GFP (A-D) or BAC2-GFP (E-H). A, E: GFP fluorescence (green); B, F: Chlorophyll autofluorescence (red); C, G: Merge of A or E with B or F, respectively; D, H: Merge of B or F with respective bright field image of the same area; Bars = 20 µm

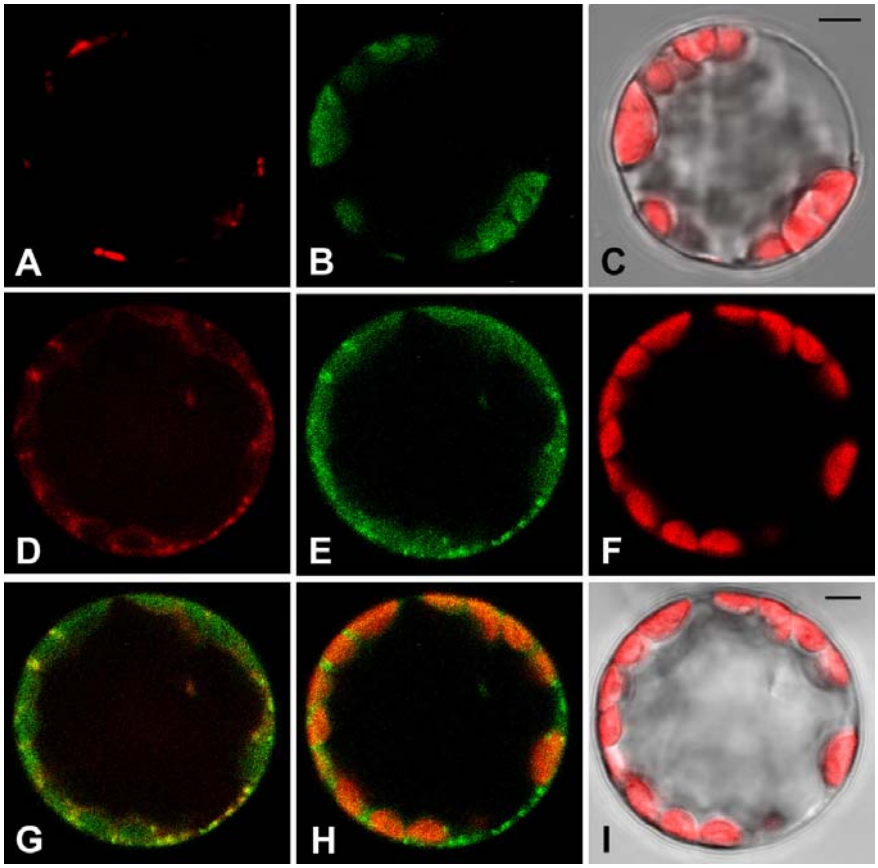

Figure 6: BAC1 is localized in mitochondria

Confocal images of MitoTracker-stained leaf mesophyll protoplasts from wild-type (A-C) in comparison to mesophyll protoplasts from a BAC1-GFP expressing plant (D-I) A, D: MitoTracker fluorescence (orange); B, E: GFP fluorescence (green); C: Merge of Chlorophyll autofluorescence (red) with bright field image of the same focal plane of the wild-type protoplast; F: Chlorophyll autofluorescence (red); G: Merge of D and E, demonstrating co-localization of BAC1-GFP with MitoTracker, indicating localization of BAC1 in the mitochondrial matrix; H: Merge of E and F demonstrating that BAC1-GFP fluorescence does generally not co-localize with chloroplasts; I: Merge of F with bright field image of the same focal plane of protoplast expressing an BAC1-GFP fusion protein; Bars = 5 µm

Because of low expression of the GFP fusion proteins and accordingly high gains for imaging, confocal images of BAC1-GFP and BAC2-GFP always showed fluorescence in the chloroplast, even when looking at the protoplasts in the GFP channel (Figure 6 E and Figure 7 E). Up to date a dual targeting to mitochondria and chloroplasts is described of approximately 50 proteins in different species (Berglund *et al.*, 2009), also for members of the MCF (Bahaji *et al.*, 2011).

However, wild-type protoplasts also showed similar fluorescence intensities of chloroplasts in the GFP channel (Figure 6 B and Figure 7 B). Therefore a dual targeting of BAC1 and BAC2 to mitochondria and chloroplast seemed unlikely, but could not be definitely excluded.

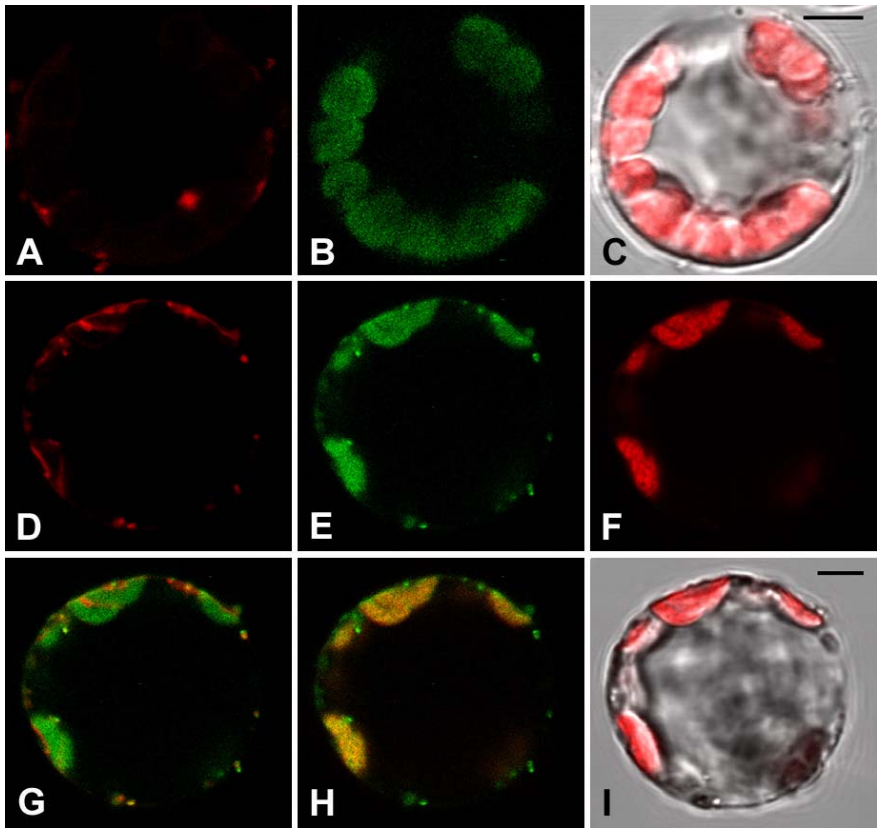

Figure 7: BAC2 is localized in mitochondria

Confocal images of MitoTracker-stained leaf mesophyll protoplasts from wild-type (A-C) in comparison to mesophyll protoplasts from a BAC2-GFP expressing plant (D-I) A, D: MitoTracker fluorescence (orange); B, E: GFP fluorescence (green); C: Merge of Chlorophyll autofluorescence (red) with bright field image of the same focal plane of the wild-type protoplast; F: Chlorophyll autofluorescence (red); G: Merge of D and E, demonstrating co-localization of BAC2-GFP with MitoTracker, indicating localization of BAC2 in the mitochondrial matrix; H: Merge of E and F demonstrating that BAC2-GFP fluorescence does generally not co-localize with chloroplasts; I: Merge of F with bright field image of the same focal plane of protoplast expressing an BAC2-GFP fusion protein; Bars = 5 µm

To specifically address a potential dual localization in mitochondria and plastids, spectral images of BAC1-GFP and BAC2-GFP expressing protoplasts were analysed by linear unmixing. Reference spectra of GFP, chlorophyll autofluorescence and autofluorescence of the cell wall were used to fit the spectral images (for detailed methodology see Chapter 4.3). The resulting images show a clear targeting of BAC1-GFP

and BAC2-GFP exclusively to mitochondria and not to chloroplasts (Figure 8 and Figure 9). Hence dual targeting of BAC1-GFP or BAC2-GFP to mitochondria and chloroplasts is very unlikely for these two membrane proteins.

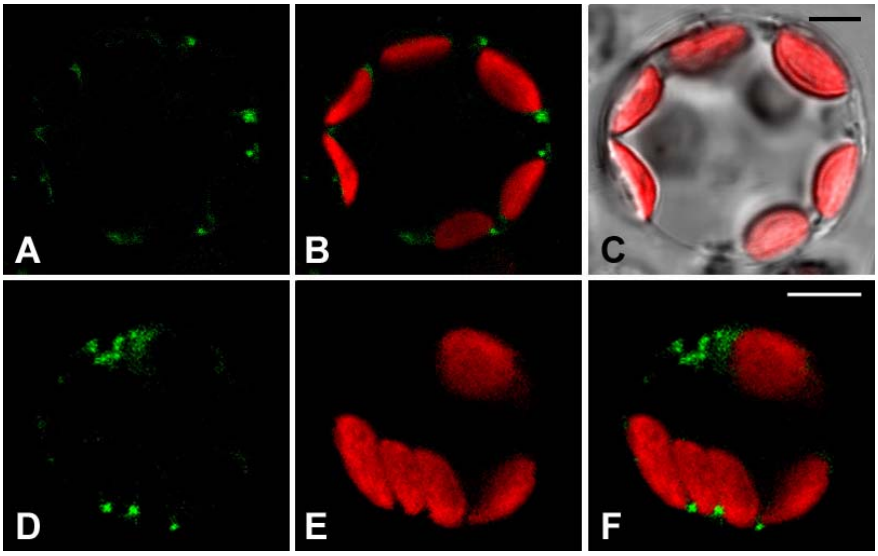

Figure 8: BAC1 is localized in mitochondria and not in chloroplasts

Intracellular localization of BAC1-GFP in leaf mesophyll protoplasts analysed by linear unmixing of confocal spectral images. A, D: GFP fluorescence (green) extracted from a lambda stack between 502 and 641 nm; B, F Merge of GFP (green) and chlorophyll autofluorescence image (red) of the same spectral image, demonstrating that BAC1-GFP is not detectable in chloroplasts; C: Merge of chlorophyll autofluorescence with bright field image of the same focal plane; E: Chlorophyll autofluorescence (red) of the same spectral image of D; Bars = 5 µm

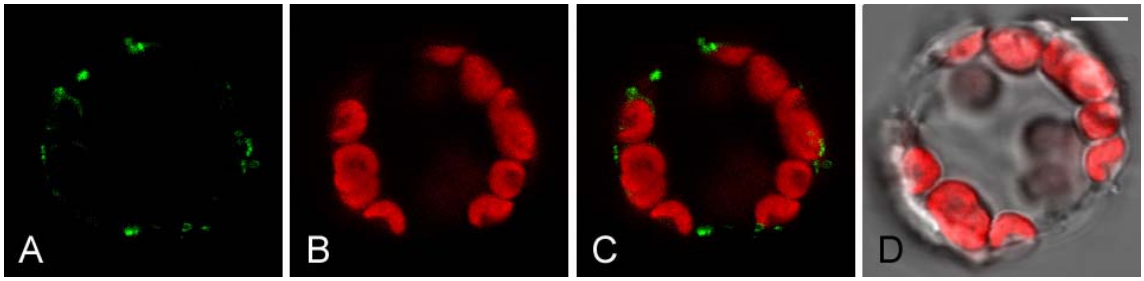

Figure 9: BAC2 is localized in mitochondria and not in chloroplasts

Intracellular localization of BAC2-GFP in leaf mesophyll protoplasts analysed by linear unmixing of confocal spectral images. A: GFP fluorescence (green); B: Chlorophyll autofluorescence (red) of the same spectral image of A; C: Merge of A and B, demonstrating that BAC2-GFP is not detectable in chloroplasts; D: Merge of chlorophyll autofluorescence with bright field image of the same focal plane; Bars = 5 µm

The experimental verification of the predicted mitochondrial localization of BAC1 and BAC2 raises the question of their function and importance in this subcellular compartment. The structural features of BAC1 and BAC2 indicate for both to be carriers for basic amino acids (Picault *et al.*, 2004). This is supported by their ability to complement the yeast *arg11* mutant (Catoni *et al.*, 2003; Hoyos *et al.*, 2003) and their transport properties assayed *in vitro* (Hoyos *et al.*, 2003; Palmieri *et al.*, 2006). The transport characteristics of BAC1 and BAC2 resemble each other, as they transport arginine, lysine, ornithine and histidine in order of decreasing affinity by both uniport and exchange. They are inactivated by the same inhibitors and their K_m and V_{max} values are very close for their most efficiently transported and preferred substrate arginine (Palmieri *et al.*, 2006).

bac2 mutants showed a strong phenotype as they grew more slowly on arginine as sole source of nitrogen than the wild-type. BAC2 overexpressors showed the opposite phenotype and grew faster than the wild type on arginine as sole source of nitrogen. These observations indicate a correlation of the expression of BAC2 with the ability to use arginine as sole source of nitrogen. Presumably, the expression of BAC2 is a limiting factor for mitochondrial arginine transport *in vivo* (Toka *et al.*, 2010), supporting the argument for arginine as preferred substrate for the BAC transporters. This is consistent with the higher expression levels of BAC2 in wild type seedlings growing on arginine as sole source of nitrogen (Catoni *et al.*, 2003).

Since *bac2* mutants did not show any phenotypical differences to the wild type when growing on soil, it is supposable, that BAC2 is not the main transporter for arginine to mitochondria during vegetative growth (Toka *et al.*, 2010). The genetic redundancy between BAC1 and BAC2 indicates that another carrier, potentially BAC1, might be responsible for mitochondrial arginine import during plant growth (Catoni *et al.*, 2003; Hoyos *et al.*, 2003; Toka *et al.*, 2010). So far nothing is known about *bac1* knock-out mutants or phenotypes of BAC1 overexpressing plants, leaving this point speculative.

RT-PCR and promotor GUS-fusions showed that BAC2 is mostly expressed in stamens and pollen grains of flowers. Only low or no expression levels of BAC2 were found in seeds and seedlings (Hoyos *et al.*, 2003; Toka *et al.*, 2010) of Arabidopsis. In many plant species arginine is the most important storage form of nitrogen in seeds and seedlings (VanEtten *et al.*, 1963; King and Gifford, 1997). Storage of nitrogen in form of arginine is also conceivable for Arabidopsis seeds, since the total arginase activity increased up to

10-fold from 0-6 days after germination (DAG) accompanied by increases in free arginine and urea levels (Zonia *et al.*, 1995). These observations indicate that also Arabidopsis seedlings need to convert stored arginine in seeds for nitrogen recycling. Arginase is localized in mitochondria (Flores *et al.*, 2008) and initiates the release of nitrogen from arginine. This means that large amounts of arginine have to be transported into mitochondria by the BAC carriers during early seedling development. The low expression of BAC2 in seeds and seedlings argues against a prominent function of BAC2 in storage mobilisation during this phase, indicating that another transporter, probably BAC1 mediates the import of arginine into mitochondria during early seedling development. This suggestion is supported by RT-PCR analysis of BAC1 with high expression in seedlings from 0-10 DAG (Hoyos *et al.*, 2003; Palmieri *et al.*, 2006). So far no expression studies for BAC1 were performed using promoter GUS-fusions, which would provide more detailed information about the tissue distribution of BAC1.

Citrulline is transported with second best affinity by BAC2, but not by BAC1 (Hoyos *et al.*, 2003; Palmieri *et al.*, 2006). Based on substrate specificities and transcript levels and assuming a nitric oxide synthase (NOS) or NOS-like protein in mitochondria of Arabidopsis, Palmieri *et al.* (2006) proposed that BAC2 catalyses the export of citrulline, a product of NOS, from mitochondria to the cytosol. Supporting this suggestion, BAC2 is strongly upregulated under stress conditions (Toka *et al.*, 2010), indicating a higher demand of citrulline transport under stress conditions. NO plays an important role for abiotic stress responses (Neill *et al.*, 2008) as well as for seed germination and seedling development (Beligni and Lamattina, 2000; Bethke *et al.*, 2004; Correa-Aragunde *et al.*, 2004). NOS-like activity, converting arginine to citrulline and NO, has been observed in plants, but the actual enzyme and its subcellular localization remain elusive (Crawford *et al.*, 2006; Gupta *et al.*, 2011). However, a NOS protein was identified the green algae *Ostreococcus tauri* (Foresi *et al.*, 2010). Assuming BAC2 to be responsible for export of the NOS product citrulline and BAC1 being involved in arginine transport for nitrogen recycling and induction of arginase activity upon germination (Palmieri *et al.*, 2006), it can by hypothesized, that the slowly growing phenotype of *bac2* mutants on arginine as sole source of nitrogen is based on disabled NO-signalling, because of the interrupted transport and therefore accumulation of citrulline in the mitochondria. This suggestion is supported by the opposite phenotype of BAC2 overexpressing plants indicating an enhanced NO-signalling and therefore better growth.

In addition to arginine, both BAC1 and BAC2 transported ornithine and lysine (Hoyos *et al.*, 2003; Palmieri *et al.*, 2006). Arginine and ornithine, as well as lysine, can be precursors for polyamines (putrescine, spermidine and spermine) and cadaverine, belonging to the polyamine group (Buchanan *et al.*, 2006). Mitochondrial ornithine and lysine need to be exported of the mitochondrial matrix probably by BAC1 and BAC2, if both amino acids are contributing to polyamine synthesis. Taking into account that polyamines are involved in the NO balance in plants, the role of BAC1 and especially BAC2 in NO production and signalling should be further investigated. Increasing levels of the polyamines spermine and spermidine induce NO release, but the reaction mechanism and cellular localization are still unknown. Polyamine-mediated NO production is involved in different developmental processes as well as in plant defense mechanisms and stress responses (Gupta *et al.*, 2011; Brauc *et al.*, 2012; Shi *et al.*, 2013). So far all analyzed proteins of polyamine biosynthesis were identified or predicted as plastid localized (ADC: Borrell *et al.* (1995), LCD: Bunsupa *et al.* (2012)), or, as in case of ornithine decarboxylase (ODC), found to be absent in the Arabidopsis genome (Hanfrey *et al.*, 2001), leaving the contribution of mitochondrial ornithine and lysine as well as the possible influence of the BAC carriers on polyamine synthesis speculative.

Focussing again on arginine as the preferred substrate of both carriers, a further question is raised beyond the transport of this amino acid. The biosynthetic pathway of arginine in plants is plastidial (Slocum, 2005). Arginine has to be transported out of the chloroplast and into mitochondria for catabolism by arginase to urea and ornithine. Since BAC1 and BAC2 were both demonstrated to be exclusively localized in mitochondria (Figure 6 and Figure 7), the export of arginine from the chloroplast must be mediated by another transporter in the plastidial inner membrane. The recently described pre-protein and amino acid transporter family (PRAT) is discussed to play role in amino acid transport in chloroplasts (Murcha *et al.*, 2007; Pudelski *et al.*, 2010), but so far nothing is known about their substrates or transport characteristics. A special arginine exporter or basic amino acid carrier like the BACs in chloroplasts was not described up to date.

With the start of this study the localization of BAC1 and BAC2 was not experimentally verified. In the meantime Toka *et al.* (2010) showed mitochondrial localization of BAC2. This study shows for the first time also for BAC1 cellular localization in mitochondria. ARGAH1 and ARGAH2 are adjacent enzymes to the BAC carriers, which process the mobilised arginine further inside the mitochondria. Quite often, metabolic enzymes in a

common pathway interact also physically, to increase the efficiency of substrate delivery and therefore flux through the pathway. It is therefore worthwhile to investigate the interaction of ARGAH1 and ARGAH2 with other mitochondrial enzymes to learn more about the interplay among these proteins.

2.2. ARGAH1 and ARGAH2 form homo- and hetero-oligomers

In many cases, protein oligomerisation is essential in regard to functional control of proteins. Arginases, purified and characterized from different plant species, showed varied sizes of monomers and homo-oligomers. In this study, Y2H assays as well as co-purification were applied to investigate the oligomerisation state of arginase from Arabidopsis, which has not been analysed so far.

2.2.1. Homology studies and structure modelling

Freely available genome databases were analysed for arginase sequences from different species (see Chapter 4.4). Sequence alignments between the plant arginases showed a high degree of amino acid sequence identity over almost the entire length of the polypeptide. The N-termini, which constitute the mitochondrial transit peptide, showed the greatest sequence diversity between the plant arginases. Aside from the conserved residues of the catalytic centre, alignments of plant and non-plant arginases showed only a low degree of similarity. Based on X-ray structures of rat and human arginases, six invariant histidine and aspartate residues are known that coordinate the Mn^{2+}-cofactor. The sequence alignments showed that these residues are also conserved in Arabidopsis Argah1 and Argah2 (Figure 10).

In human arginase 1, Glu256 and Arg255 are required for the trimeric oligomerisation of the monomers (Sabio *et al.*, 2001). Glu256 appears to be replaced by a similarly positioned aspartate in plant arginases (Asp294 in ARGAH1 and Asp296 in ARGAH2) not changing the polarity at this position. Arg255 is conserved in all analysed sequences, except the Synechocystis arginase (Arg293 in ARGAH1 and Arg295 in ARGAH2). Analysis of sequence alignments (Figure 10) and structure modelling (Figure 11) showed that the residues required for cofactor binding and special orientation of the catalytic

centre as well as the residues for oligmerisation are highly conserved between different species and kingdoms.

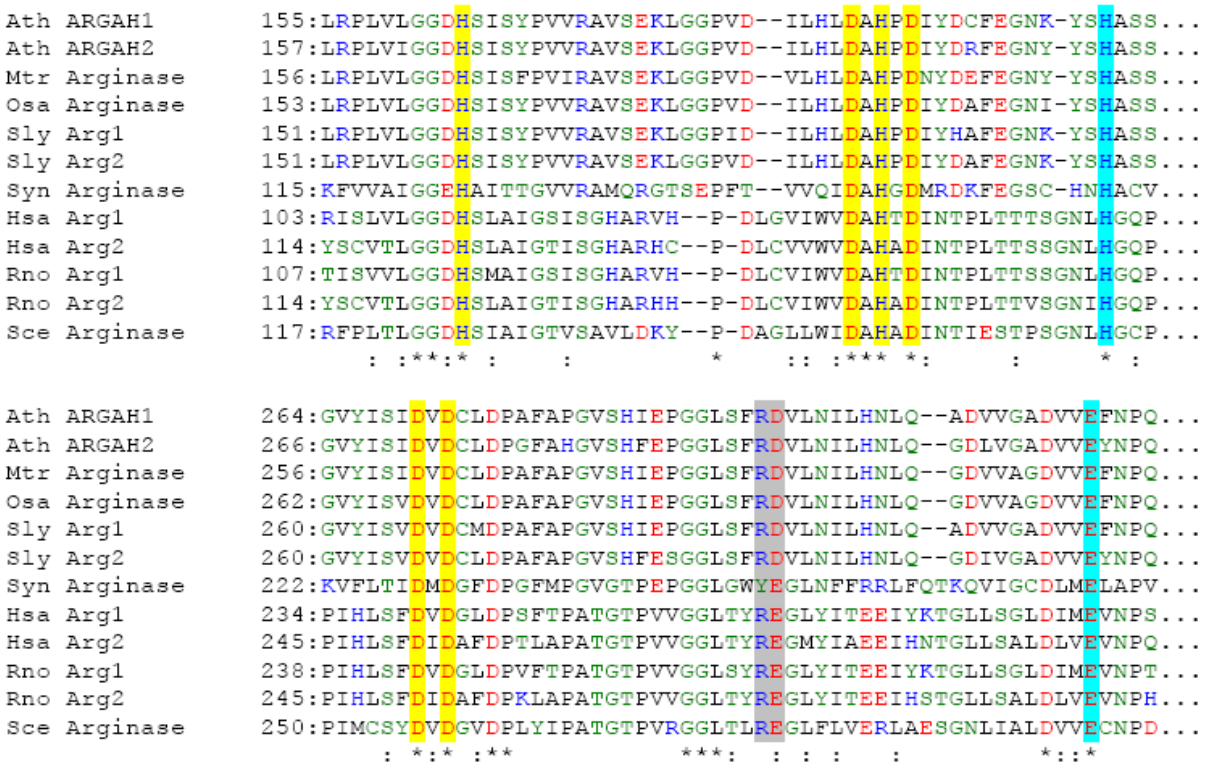

Figure 10: Multiple sequence alignment shows highly conserved amino acids in the catalytic centre of arginases from different species

Arginase protein sequences from different species were aligned by ClustalW. Amino acids involved in binding the Mn^{2+}-cofactors in the crystal structure of rat arginase 1 are highlighted in yellow. Residues highlighted in turquoise are involved in binding the substrate arginine and are conserved in vertebrates, funghi and plants, too. Amino acids known to mediate oligomerisation in human arginase 1 are shaded in gray and also show conservation. Black residues: non-polar amino acids; green residues: polar amino acids; blue residues: basic amino acids; red residues: acidic amino acids; Ath: *Arabidopsis thaliana*; Mtr: *Medicago truncatula*; Osa: *Oryza sativa* Japonica Group; Sly: *Solanum lycopersicum*; Syn Arginase: *Synechocystis* sp. PCC6803 arginase; Hsa: *Homo sapiens*; Rno: *Rattus norvegicus*; Sce: *Saccharomyces cerevisiae* S288c. * indicates 100 % conservation, : indicates homologous exchange at the given position

For computational structural analysis of ARGAH1 and ARGAH2, both structures were modelled using Phyre2 (Chapter 4.4, Kelley and Sternberg (2009)) fed with protein sequences of ARGAH1 and ARGAH2 lacking the predicted mitochondrial transit peptide. 94 % or 97 % of the residues of ARGAH1 or ARGAH2, respectively, were modelled with 90 % confidence. For modelling of both structures, arginases and agmatinases from different species were used by the Phyre2 program. Arginases and agmatinases belong to

the family of ureohydrolases, sharing the same catalytic principle. While arginase processes arginine, agmatinase uses the decarboxylated form of arginine, agmatine, demonstrating the comparability of both enzymes. However, phylogenetic analyses and homology studies showed a plant arginase cluster clearly distinguishable from other members of the arginase superfamily (non-plant arginases, plant arginases, agmatinases and agmatinase-like enzymes) (Chen *et al.*, 2004). The modelled structures were compared to the known crystal structure of rat arginase 1 regarding the general structure, including the overall fold of α-helices and β-sheets, as well as the orientation of amino acid residues in the catalytic centre (Figure 11).

The overall fold of both arginase proteins belongs to the α/β family, consisting of a central, spiralled β-sheet formed from eight parallel strands and flanked on both sides by numerous α-helices (Figure 11, A-F). The catalytic centre is located inside the protein as it is already known for rat arginase 1 (Figure 11, G-I). The orientation of the binuclear Mn^{2+}-cluster is shown in Figure 11 K for rat arginase 1 (Colleluori *et al.*, 2005). His141 and Glu277 (positions correspond to the rat arginase 1 enzyme) are essential amino acids for catalysis (Colleluori *et al.*, 2005) and are also conserved in the Arabidopsis arginases. Since the role of His141 in the rat arginase was investigated by mutagenesis to alanine, this residue is not visible in the structure of the catalytic centre in Figure 11 panel K.

The conserved structure of the monomers, the active site and amino acids required for oligomerisation of arginases pose the question of oligomerisation of ARGAH1 and ARGAH2. All arginases that were structurally analysed so far have a trimeric or hexameric quartenary structure, with identical tertiary structures for individual monomers (Dowling *et al.*, 2008). The high sequence similarity and the predicted structural congruence of ARGAH1 and ARGAH2 with arginases from other species suggested that also the Arabidopsis arginases form homo- or hetero-oligomers. To test this hypothesis experimentally, interactions between the Arabidopsis arginases and other enzymes of the arginine and proline degradation pathways were analysed by various approaches.

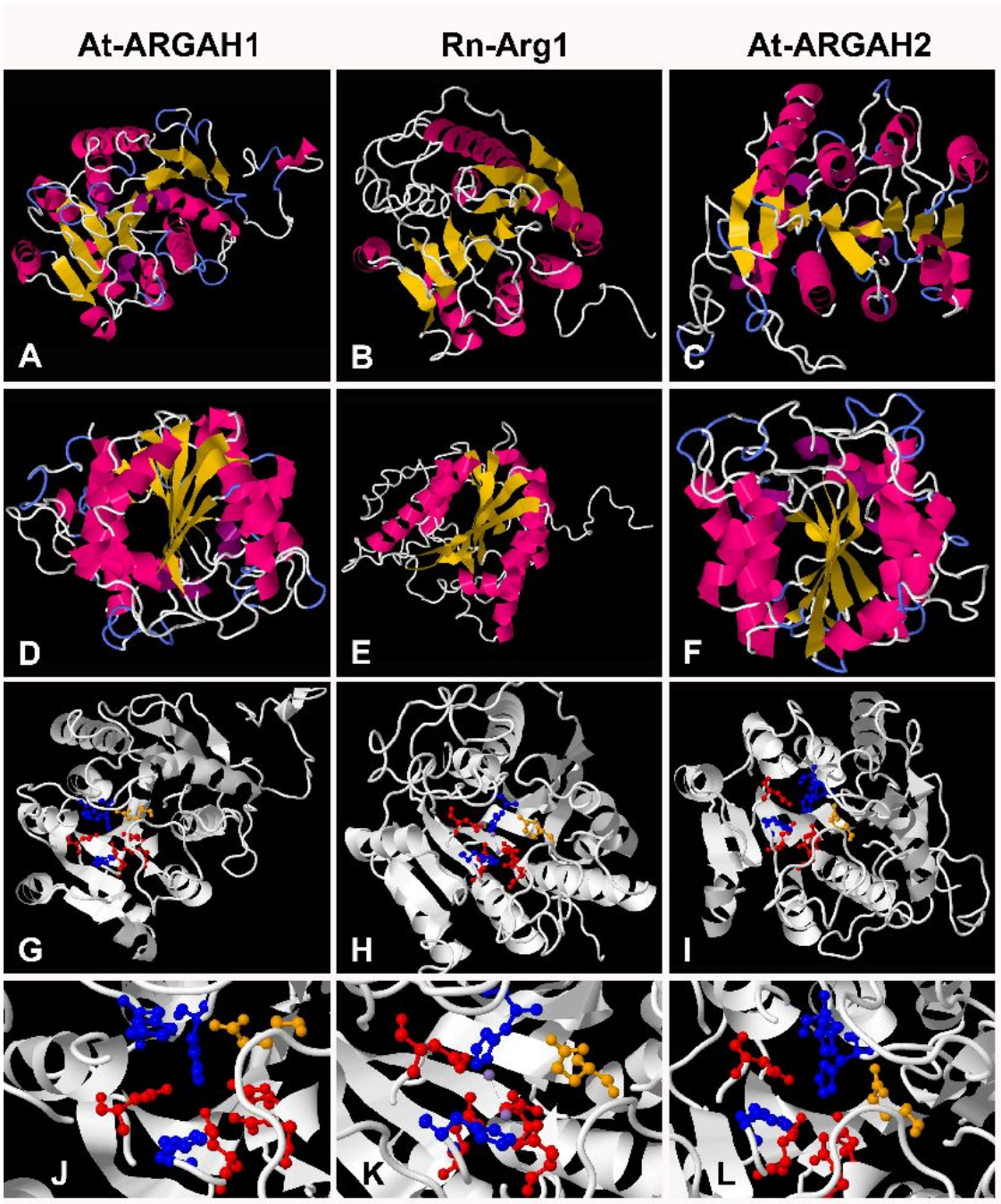

Figure 11: Modelled structures of Arabidopsis ARGAH1 and ARGAH2 and crystal structure of rat (*R. norvegicus)* arginase 1

Structure of ARGAH1 (A,D,G,J) and ARGAH2 (C,F,I,L) were modelled using Phyre2 and compared to the known crystal structure of arginase 1 from *R. norvegicus* (B,E,H,K). The overall fold of α-helices and β-sheets as well as the orientation of the Mn^{2+}-cofactor binding site are very similar, demonstrating the conserved catalytic centre. All coloured residues are required for Mn^{2+}-cofactor binding or substrate binding. Blue: histidine, red: aspartate, orange: glutamate. The third histidine of the catalytic centre was mutated to alanine in *R. norvegicus* arginase 1 and is therefore not visible in panel K.

2.2.2. Oligomerisation studies

For the analysis of protein-protein interactions of Arabidopsis arginases, a Y2H assay was set up with ARGAH1 and ARGAH2 as bait and prey. Each fusion construct was first expressed alone in *S. cerevisiae* and expression was verified by immunoblotting using an antiserum raised against loblolly pine arginase (Todd and Gifford, 2002) (Figure 12).

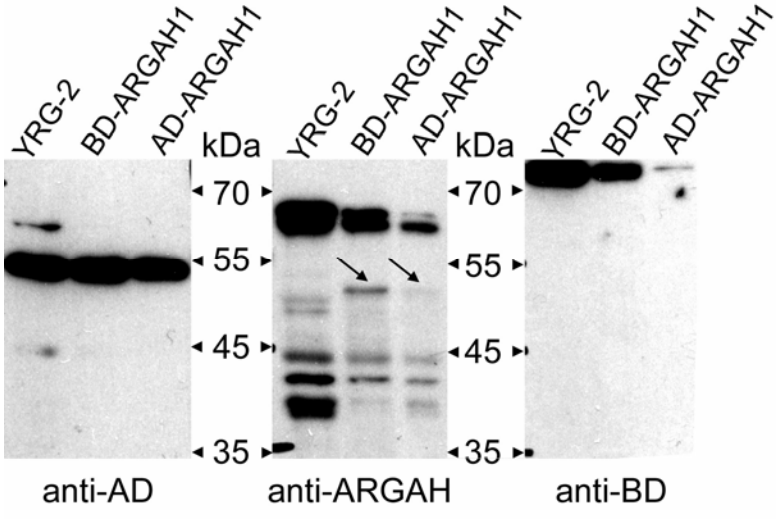

Figure 12: Expression of BD-ARGAH1 and AD-ARGAH1 fusion proteins in yeast

Example of immunoblots of soluble protein extracts from YRG-2 yeast cells expressing the fusion proteins BD-ARGAH1 (56 kDa) or AD-ARGAH1 (54 kDa) in comparison to the untransformed host strain without any fusion proteins. BD-ARGAH1 and AD-ARGAH2 fusion proteins are detected by an anti-arginase antierum (arrows), but not by commercial polyclonal peptide antibodies against the activation domain (AD) or binding domain (BD) of Gal4. Antibodies: anti-AD: anti-GAL4 activation domain (1:2000), anti-BD: anti-GAL4 DNA-binding domain (1:2000), anti-ARGAH serum (1:5000).

However, detection with commercial antibodies against the DNA-binding domain (anti-GAL4-DNA-BD) or the activation domain (anti-GAL4-AD) never succeeded independent of the protein extraction protocol or the antibody concentration.

Subsequently, the fusion constructs were co-expressed in the *S. cerevisiae* strain YRG-2 in every possible AD/BD combination and tested for their ability to activate expression of the *HIS3* reporter gene, which is indicative for a physical interaction of the heterologously expressed proteins (Figure 13). No complementation of His-auxotrophy was observed when the reporter strain was co-transformed with BD-Argah1 or BD-Argah2 constructs together with the empty AD-vector (Figure 13, row 3). Likewise, the AD-Argah-constructs together with the empty BD-vector showed no complementation,

thus excluding self induced activation of the *HIS3* reporter gene by ARGAH proteins (Figure 13, column 3).

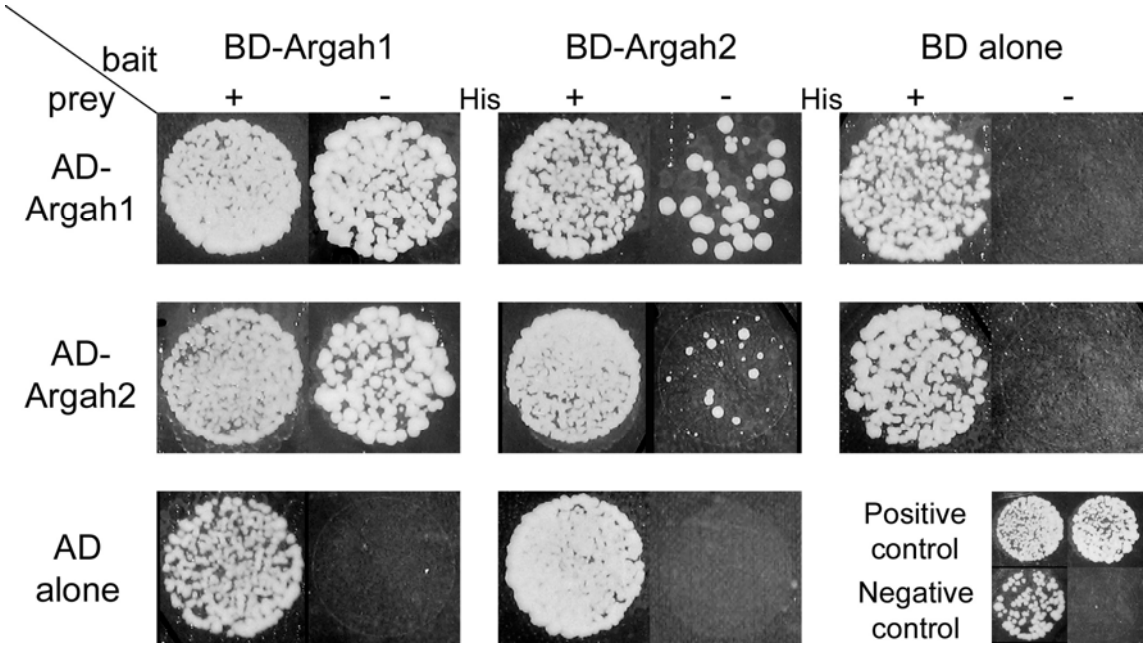

Figure 13: Y2H assay of ARGAH1 and ARGAH2 indicating homo- and hetero-oligomerisation of the two arginase isoforms from Arabidopsis

Each array shows growth of yeast colonies containing a bait vector (BD, indicated at the top) and prey vector (AD, indicated at the left side) on synthetic complete dropout (SC)-agar with His (plating control, left spot) or without His (interaction test, right spot). Empty bait and prey vectors are used as controls for self-induced activation. The assay was repeated twice with three independent replicates and identical results were obtained in each instance. AD: activation domain of *S. cerevisiae* GAL4; BD: DNA-binding domain of *S. cerevisiae* GAL4.

The combinations BD-ARGAH1/AD-ARGAH1 and BD-ARGAH1/AD-ARGAH2 resulted in full complementation of His-auxotrophy, indicating a strong interaction between the bait and the prey proteins (Figure 13, column1) and therefore suggesting that ARGAH1 forms stable homo-oligomers and hetero-oligomers with ARGAH2. The combination BD-ARGAH2/AD-ARGAH1 showed weaker activation of the *HIS3* reporter gene (Figure 13, column 2, row 1) as compared to the inverse combination, indicating that the spatial positioning of the AD- and BD-domains influences the outcome of the assay. However, it remains to be determined whether the very low level activation of the *HIS3* reporter gene by homo-oligomerisation of ARGAH2 (Figure 13, column 2, row 2) indicates only a

weak interaction within the homo-oligomeric complex or is due to poor accessibility of the AD and/or BD domains.

Investigation of proteins targeted to plant mitochondria in the nucleus based Y2H system comprises the general risk of false positive results and therefore a detected interaction need to be verified by an independent method like a bimolecular fluorescence complementation (BiFC) assay or a co-purification assay.

Verification of the interaction of ARGAH1 and ARGAH2 as homo- and hetero-oligomers by reconstitution of YFP in a BiFC assay (Chapter 4.10) was so far not successful. Tobacco leaves were transiently co-transformed with constructs for overexpression of ARGAH1 fused to either the N-terminal or the C-terminal half of YFP and expression of the fusion proteins was confirmed by western blotting (Figure 15 A). However, no YFP fluorescence could be detected by fluorescence microscopy, even if co-transformation with constructs for full length GFP and CFP targeted to mitochondria clearly demonstrated co-expression of both fluorescent proteins in the majority of the transformed cells (Figure 14).

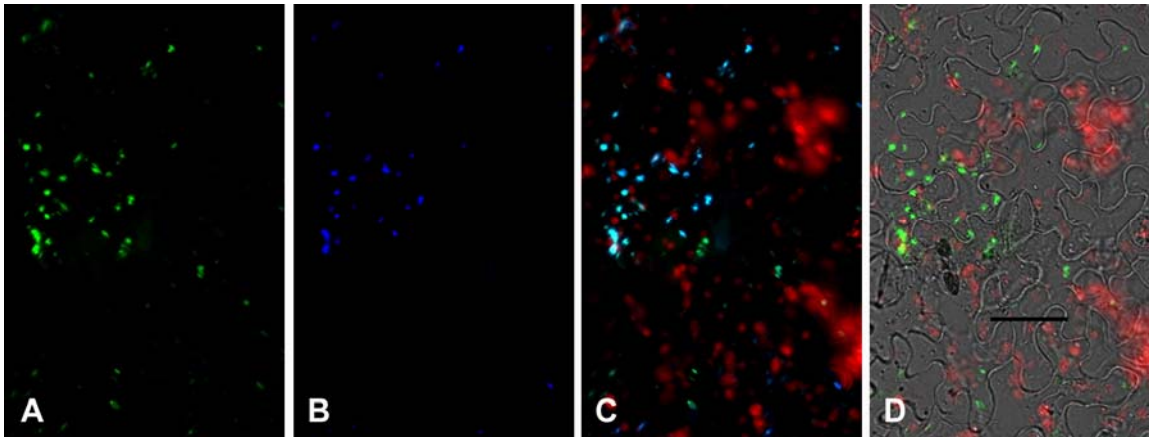

Figure 14: Co-transformation with full length GFP and CFP targeted to mitochondria

Transiently co-transformation of *N. benthamiana* with constructs for full length GFP and CFP targeted to mitochondria (mitochondrial transit peptide of proline dehydrogenase fused to full length GFP or CFP) clearly demonstrated co-expression of both fluorescent proteins in the majority of the transformed cells. A: GFP fluorescence (green), B: CFP fluorescence (blue), C: Merge of A and B and chlorophyll auto fluorescence (red) image of the same focal plane, D: Merge of A, chlorophyll auto fluorescence (red) and a bright field image of the same focal plane. Bars: 20 µm

Because of the successful co-expression of full-length GFP and CFP proteins it is very unlikely that the reconstitution of the split YFP was prevented by problems with co-transformation or mitochondrial import. More likely, the lacked YFP reconstitution is due misfolded fusion proteins in mitochondria or special positioning problems of the C-terminally attached split-YFP-fragments. Oligomerisation of the arginase monomers occurs most likely with participation of Arg293 and Asp294 (ARGAH1: Arg293, Asp294; ARGAH2: Arg295, Asp296) arranging the C-terminus to stick out in the centre of the monomer orthogonal to the plain of the trimer (Figure 15 B). Therefore, accessibility of the split-YFP fragments is unlikely to be restricted in a potential oligomer. However, the 20 amino acid linker between the arginase monomer and the YFP fragment may be too short to provide the necessary flexibility of the split-YFP fragments needed for reconstitution. Improving the flexibility by addition of up to ten amino acids will probably lead to confirmation of the homo- and hetero-oligomerisation by BiFC.

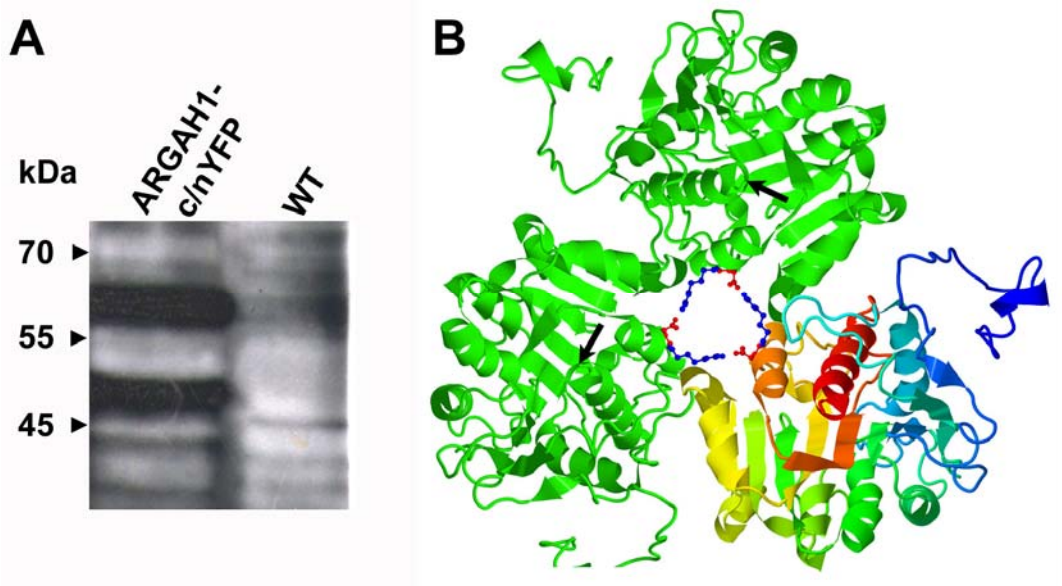

Figure 15: BiFC fusion proteins are expressed in *N. benthamiana*

A: ARGAH1-cYFP (46 kDa) and ARGAH1-nYFP (59 kDa) were co-expressed in transiently transformed *N. benthamiana*. Detection: anti-arginase, 1:5000, WT: untransformed control leaf, B: potential trimer of Arabidopsis ARGAH1 arranged from the modelled monomer (green or rainbow colour, blue: N-terminus, red: C-terminus) with highlighted Arg293 (blue) and Asp294 (red) residues probably required for oligomerisation. The C-terminus is red coloured or indicated by arrows in the green coloured monomers and demonstrates the potential special positioning of the split-YFP fragments for BiFC assays

For the co-purification assay, ARGAH1 tagged with a C-terminal Strep-tag and ARGAH2 with an N-terminal His-tag, were co-expressed in *E. coli* and purified using affinity chromatography to capture one of both isoforms. Immunoblots using an 5 x His-antibody or Strep-Tactin horseradish peroxidase conjugate (HRP) showed co-purification of both isoforms in identical elution fractions of a Ni-NTA column that captures selectively the 6 x His-tag, verifying hetero-oligomerisation of ARGAH1 and ARGAH2 (Figure 16). The co-purification assay was performed twice with the identical results. Also capturing the Strep-tagged ARGAH1 on a StrepTactin resin yielded both isoforms in the elution fractions (data not shown). To ensure that the co-purification was not due to nonspecific interactions, Strep-tagged ARGAH1 was subjected to Ni-NTA affinity chromatography. In this case, all ARGAH1 was detected in the flow through and none in the elution fractions (data not shown).

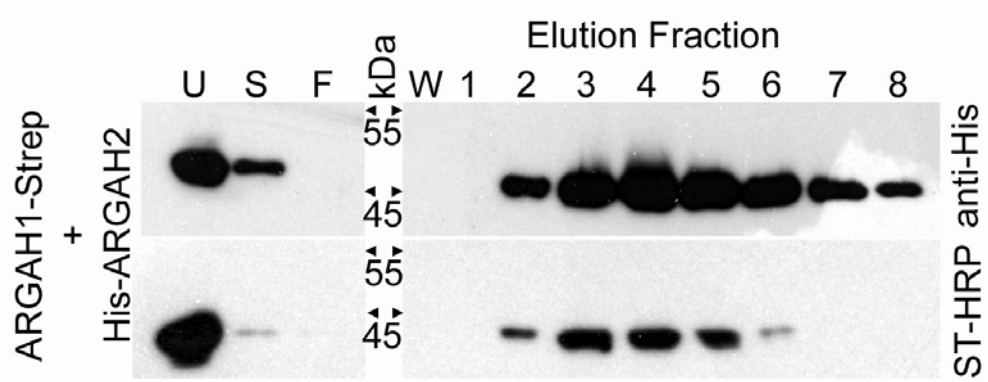

Figure 16: Co-purification assay of ARGAH1 and ARGAH2 confirming hetero-oligomerisation of the arginase isoforms

Immunoblot of ARGAH1-Strep/His-ARGAH2 co-expressed in *E. coli* and purified by Ni-NTA affinity chromatography. ARGAH1-Strep was co-purified because of hetero-oligomerisation with ARGAH2. For detection of ARGAH1-Strep and His-ARGAH2 a Strep-Tactin HRP conjugate or His-antibody HRP conjugate was used, respectively. U: unsoluble fraction of protein preparation; S: soluble fraction of protein preparation that was used for affinity chromatography; F: Flowthrough of affinity chromatography; W: Wash fraction of affinity chromatography; ST-HRP: Strep-Tactin horseradish peroxidase conjugate (1:100000); anti-His: His antibody HRP conjugate (1:10000)

Based on the known arginase structures from other organisms and the modelled structure of ARGAH1 and ARGAH2, a homo-trimeric structure can also be proposed for the Arabidopsis arginase isoforms. Results from the Y2H assay confirm homo-oligomeric structures at least for ARGAH1 but do not give any information about the number of monomers per oligomer. Investigating the molecular mass of the complex and monomers

by size exclusion chromatography and subsequent activity assays will further elucidate of the structure of Arabidopsis ARGAH1 and ARGAH2 homo- and hetero-oligomers.

Although the formation of mixed multimers of ARGAH1 and ARGAH2 was proposed already by Flores *et al.* (2008), hetero-oligomerisation of arginase isoforms was not experimentally demonstrated in any organism so far. In addition to the observed interaction of the arginase isoforms in this study, hetero-oligomerisation is conceivable with regard to amino acid identity as well as results of phylogenetic and expression studies. The Arabidopsis arginase isoforms are overall 86 % identical on the amino acid level (Flores *et al.*, 2008). The N-terminal region encoding the mitochondrial transit peptide shows the highest degree of divergence. Phylogenetic analyses indicate that the duplication of *Argah1* and *Argah2* occurred independently from other duplications of plant arginases (Chen *et al.*, 2004; Brownfield *et al.*, 2008), suggesting that only a slight sub-functionalisation of the arginase isoforms has evolved so far. This is supported by redundant expression patterns in the vasculature of roots, cotyledons and in actively growing tissues analysed by promotor-GUS fusion constructs (Brownfield *et al.*, 2008; Flores *et al.*, 2008), indicating that the formation of mixed oligomers is possible in these tissues. Only ARGAH1 shows a slightly sub-functionalisation because of exclusive expression in pollen and in hypocotyls of three day-old seedlings (Brownfield *et al.*, 2008). The combination of arginase expression patterns and the interaction of both isoforms presented in this study point to different monomer compositions of arginase oligomers. Even if the oligomerisation of ARGAH1 and ARGAH2 needs to be further investigated, it is conceivable that homo- and hetero-oligomeric complexes display different arginase activities. ARGAH2 displays the major arginase activity, whereas ARGAH1 accounts for at most 25 % of arginase activity in three day-old seedlings (Flores *et al.*, 2008). Different compositions of homo- and hetero-oligomers could present a novel way to regulate arginase activity in different tissues or in response to environmental changes.

The function of arginase, catalyzing the hydrolysis of arginine, mobilizes nitrogen in form of urea and ornithine within mitochondria. Urea then leaves the mitochondria and is hydrolysed by cytosolic urease (Witte, 2011). The released ammonium is re-assimilated by cytosolic glutamine synthetase (GS1) (Witte, 2011). Ornithine is either transported back into plastids for regeneration of arginine or, which is more likely, is processed by the mitochondrial ornithine δ-aminotransferase (δOAT). δOAT transfers the δ-amino group of ornithine to α-ketoglutarate generating one molecule of glutamate

and Δ^1-pyrroline-5-carboxylate (P5C). P5C is subsequently oxidized to a second molecule of glutamate by P5CDH. Sharing the same intermediate, P5C, proline and arginine catabolism are linked by δOAT (Roosens *et al.*, 1998; Funck *et al.*, 2008).

Since P5C is a chemically unstable molecule (Williams and Frank, 1975) and induces cell death when accumulated (Deuschle *et al.*, 2004), it is very unlikely that δOAT releases this intermediate product into the mitochondrial matrix. It seems more likely that δOAT and P5CDH form transient protein complexes (Elthon and Stewart, 1982; Funck *et al.*, 2008). Investigating the interaction characteristics and the physiological role of δOAT provides detailed information about the second enzyme of arginine breakdown.

2.3. δOAT interaction characteristics and its role in plant physiology

The formation of reversible enzyme complexes of δOAT and P5CDH, exchanging P5C without releasing it to the mitochondrial matrix, was discussed already by Elthon and Stewart (1982) and Funck *et al.* (2008). For investigation of interactions between δOAT and P5CDH with each other as well as with other enzymes of proline and arginine catabolism, interactions were assayed pairwise using a yeast-two-hybrid (Y2H) system.

2.3.1. Interactions between enzymes of proline and arginine catabolism

The interaction characteristics of Arabidopsis δOAT were analysed by setting up a Y2H assay with distinct combinations of enzymes of the arginine and proline catabolism as bait and prey (Table 1).

The Y2H assay did not provide evidence for an interaction of δOAT including the mitochondrial transit peptide with any of the tested candidates, neither with enzymes of proline catabolism nor with enzymes for arginine degradation (Table 1). Regarding the arrangement of the fusion proteins, the AD- or BD-domain are N-terminally fused to the bait or prey making N-terminal processing impossible. This again means that the fusion proteins including a mitochondrial transit peptide are transported to the nucleus of the yeast cells, leading to potential folding problems. Additionally, both the GAL4-domains and the unprocessed transit peptides may sterically hinder the interaction between the candidate proteins. Regarding this problem, δOAT and P5CDH fusion proteins lacking

the potential mitochondrial transit peptide were also tested for interaction. However, the Y2H assays with the truncated versions of δOAT and P5CDH did also not provide evidence for interaction (Table 1).

Table 1: Interactions studies with enzymes of arginine or proline catabolism

Summary of all tested combinations of arginine and proline degradation enzymes in Y2H assays, illustrating that δOAT seems not to be involved in an enzyme complex preventing P5C from being released to the mitochondrial matrix. Empty bait (DNA-BD-GAL4) and prey (AD-GAL4) vectors are used as controls for self-induced activation. Each assay was repeated two times with three independent biological replicates. Green array +: interaction observed; yellow array +: weak interaction observed; -: no interaction observed; grey array: combination was not tested, -fl: full length protein including the mitochondrial transit peptide, -N##: protein lacking the ## N-terminal amino acids containing at least the predicted mitochondrial transit peptide (predicted by MitoProt: http://ihg.gsf.de/ihg/mitoprot.html)

		δOAT			P5CDH			ProDH	ARGAH1	ARGAH2	DNA-BD-GAL4
		-fl	-N48	-N102	-fl	-N39	-N75	-fl	-fl	-fl	
δOAT	-fl	-			-	-	-	-	-	-	-
	-N48		-		-	-	-	-	-	-	-
	-N102			-	-	-	-	-	-	-	-
P5CDH	-fl	-	-	-	-			-			-
	-N39	-	-	-		+					-
	-N75	-	-	-			+				-
ProDH	-fl	-	-	-	-			-			-
ARGAH1	-fl	-	-	-					+	+	-
ARGAH2	-fl	-	-	-					+	+	-
AD-GAL4		-	-	-	-	-	-	-	-	-	

These results suggest δOAT not to be involved in an enzyme complex with P5CDH. However, the Y2H assays revealed a homo-oligomerisation of P5CDH when the protein was expressed without the mitochondrial transit peptide (Table 1). Since P5CDH is a confirmed mitochondrial protein (Elthon and Stewart, 1981), these results indicate that removal of the mitochondrial transit peptide is crucial for the stability or homo-oligomerisation of P5CDH. After final folding, the P5CDH monomers are able to bind to

each other and form a homo-oligomeric complex, most probably a tetramer (Funck, 2001).

Investigating the pH-optimum of P5CDH, Elton and Stewart (1982) observed two activities with distinct pH optima at pH6.4 and pH8. Based on the pH optima of proline and ornithine dependent respiration, the authors postulated two different P5CDH isoforms, one acting on P5C produced from proline by ProDH and the other on P5C generated by δOAT activity. However, homology based sequence analysis of the maize genome revealed P5CDH as single copy gene in maize, as well as in the Arabidopsis genome (Deuschle *et al.*, 2001). The apparent conflict between a single copy gene for *P5CDH* and two distinct pH-optima of the enzymatic activity can be resolved in two different ways: Firstly, a so far unknown enzyme without homology to the known P5CDHs but with P5CDH activity may be the cause for one of both measured activities. Secondly and more likely, posttranslational modification of the P5CDH monomers, probably by protonation (Schonichen *et al.*, 2013), results in distinct oligomeric complexes each with its own pH-optimum and preferential reaction with P5C molecules coming from either ProDH or δOAT.

For further investigations, the homo-oligomerisation of P5CDH has to be verified by an additional method, for example by bimolecular fluorescence complementation (BiFC). Alternatively, purified P5CDH could be analysed for pH-dependent changes in oligomerisation by size exclusion chromatography. Additionally, isolated active P5CDH could be tested *in vitro* either with active δOAT or active ProDH. The active enzyme mixtures are supplied with ornithine or proline at a distinct pH and glutamate production is measured, giving detailed information about the activity of the proposed oligomeric states at distinct conditions.

The hypothesis of two distinct oligomerisation complexes for distinct P5C pools makes the interaction of δOAT and P5CDH even more likely, but the negative Y2H assays using these two candidates leave this point speculative, even if Y2H assay are more prone to false negative than false positive results (Bruckner *et al.*, 2009; Stellberger *et al.*, 2010).

2.3.2. Library screening reveals potential δOAT interaction partners

Since no direct interaction between δOAT and the other tested candidates could be detected, it was conceivable that the putative multi-enzyme complex might depend on a metabolically inactive scaffold protein. In order to identify so far unknown interaction partners of δOAT, a Y2H screen using δOAT as bait was performed starting with 3 x 10^5 independent clones from the Horwitz and Ma Two-Hybrid Library (ABRC, Ohio) (Table 2 A).

Starting with 556 isolated positive clones after the primary screen the majority of the clones turned out to be false positive clones after re-plating (380 clones) and re-transformation (165 clones), ending up with 11 positive clones including two proteins conferring δOat-independent activation in the Y2H assay and finally nine sequenced clones (Table 2 B). Most of the potential interactions partners were not located in mitochondria, making an interaction with δOAT *in vivo* very unlikely. The most promising candidates are TOUCH3 (*Arabidopsis thaliana* calmodulin like 4) and ASB1 (anthranilate synthase beta subunit 1), since both are predicted to be localized in mitochondria by the localization predictor AtSubP (Kaundal *et al.*, 2010).

So far, both proteins, TOUCH3 and ASB1, are not in any known relation to δOAT, neither with substrates, products, intermediates or a cofactor nor with energy equivalents like NADH or ATP. TOUCH3 is strongly upregulated in response to mechanical stimuli, such as touch and wind and encodes a calcium ion-binding protein that is closely related to calmodulin (Antosiewicz *et al.*, 1995). A reliable subcellular prediction for TOUCH3 does not exist, since an array of different algorithms predicts targeting either to the secretory pathway or to the mitochondrion (http://aramemnon.botanik.uni-koeln.de/index.ep). ASB1 is the beta subunit of anthranilate synthase and catalyzes the first step of tryptophan biosynthesis by converting chorismate and glutamine to anthranilate, pyruvate and glutamate (Niyogi *et al.*, 1993). ASB1 is strongly predicted to be localized in chloroplasts and weakly predicted to mitochondria (http://aramemnon.botanik.uni-koeln.de/index.ep).

Table 2: Results of Y2H screen with δOAT as bait and sequenced potential interaction partners

A: Estimated number of analysed clones and positive clones of each selection round of the Y2H screen using δOAT as bait (see Chapter 4.8 for detailed method). B: Sequenced positive clones after the third selection round, displaying protein name, genomic locus and subcellular localization (p: predicted; c: experimentally confirmed) compartment

A

	Amount of clones
Potential analysed clones	$3{,}0 \times 10^5$
Positive clones in the primary screen	556
Positive clones after re-plating	176
Positive clones after re-transformation	11
Self-induced activation	2
Sequenced clones	9

B

Protein	Locus	Subcellular localization
Lhcb4.3, light harvesting complex of photosystem II	AT2G40100	chloroplast (c)
PIP3, plasma membrane intrinsic protein 3	AT4G35100	plasma membrane (c)
TOUCH 3, *Arabidopsis thaliana* calmodulin like 4	AT2G41100	plasmodesma (p), vacuolar membrane (p), **mitochondrion** (p)
Disease resistance protein (TIR-NBS-LRR class)	AT5G51630	chloroplast (p) cytoplasma (p)
Homolog of human UAP56 B, (DEAD/DEAH box RNA helicase family protein)	AT5G11200	cell wall (c), plasmodesma (c), nucleus (c)
Sesquiterpene synthase	AT5G44630	chloroplast (p), plasmodesma (c)
ASB1, anthranilate synthase beta subunit 1, tryptophan biosynthesis 4	AT1G25220	**mitochondrion** (p)
chaperonin-60 alpha subunit, chaperone involved in RubisCO folding	AT2G28000	chloroplast (c)
transducin family protein / WD-40 repeat family protein	AT3G18860	cytosol (c), plasmodesma (c)

Assuming a connection of δOAT to tryptophan biosynthesis because of interaction with ASB1, the retarded growth of *δoat* mutants (Funck *et al.*, 2008) on arginine containing medium could potentially be explained by a blocked or insufficient tryptophan biosynthesis, which has essential functions additional to amino acid biosynthesis. Plants use this pathway to produce precursors for numerous secondary metabolites, including the hormone auxin, indole alkaloids, phytoalexins, cyclic hydroxamic acids, indole glucosinolates or acridone alkaloids. These metabolites serve as growth regulators, defence agents and signals for insect pollinators and herbivores (Buchanan *et al.*, 2006). Some of these alkaloids have great pharmacological value, including the anticancer drugs vinblastine and vincristine (Radwanski and Last, 1995). These compounds were not found so far in Arabidopsis, but the possibility that Arabidopsis has the capacity to synthesize and accumulate complex alkaloids is a matter of discussion (Facchini *et al.*, 2004).

For both proteins, TOUCH3 and ASB1, interaction characteristics with P5CDH will be examined, since a multi-enzyme complex of TOUCH3 or ASB1 with δOAT and P5CDH is conceivable. Even if the screen has investigated so far only 3×10^5 potential clones, which definitively should be improved by an additional screen, the detection of nine proteins that are capable to interact with δOAT in a heterologous system demonstrate that δOAT is very likely to interact with other proteins also *in vivo*. Database analysis predicted the involvement of δOAT into glutamine catabolic and glutamate metabolic processes or interaction with floral regulators (Kavi Kishor and Sreenivasulu, 2013), but so far no physical interaction of δOAT with any of the predicted proteins or enzymes of proline catabolism is known. Most alternative methods for identification of potential interaction partners of δOAT demand a highly specific antibody against δOAT which was another aim of this study.

2.3.3. A polyclonal antiserum against δOAT was raised in rabbit

In awareness of the Y2H limitations, the question of potential interaction partners of δOAT was decided to be approached by a pull down assay of native protein complexes from mitochondrial extracts. To produce an antiserum against the native δOAT protein, recombinant 6 x His-tagged δOAT lacking the mitochondrial transit peptide was expressed in *E. coli* and purified under non-denaturing conditions using Ni-NTA affinity

chromatography (His-tag purification) followed by a desalting step and anion exchange chromatography (Figure 17).

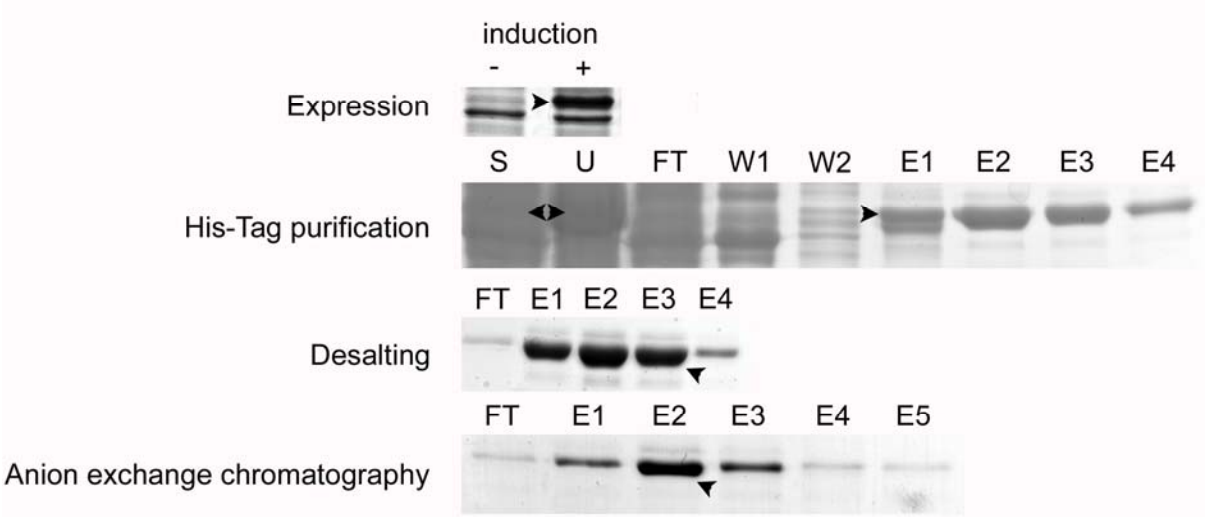

Figure 17: Purification of native δOAT using His-tag purification, desalting and anion exchange chromatography

After recombinant expression in *E. coli,* δOAT was purified using three successive purification steps: affinity chromatography (His-tag purification) followed by a desalting step and anion exchange chromatography (quartenary amine (Q)). S: soluble protein; U: unsoluble protein; FT: flow through, W: wash fraction; E: elution fraction. Proteins of each fraction were separated using SDS-PAGE and stained with Coomassie. The arrow indicates the position of δOAT.

A rabbit was immunized with the recombinant δOAT as antigen. Immunoblots using the resulting δOAT antiserum showed a highly sensitive detection of δOAT in total protein extracts of Arabidopsis as well as in *E. coli* cells expressing the recombinant protein (data not shown). Unfortunately, the serum reacted also with several other proteins, among them one with a similar size as δOAT, which could not always be clearly separated from the δOAT-specific signal but was clearly detected in protein extracts of δ*oat* knockout mutants (Figure 18). The specificity of the serum was improved by affinity purification. Recombinant P5C reductase was used for negative absorption and recombinant δOAT for positive absorption. The δOAT-specific antibodies were concentrated and unspecific signals were reduced, but the one with a similar size as δOAT was still detectable.

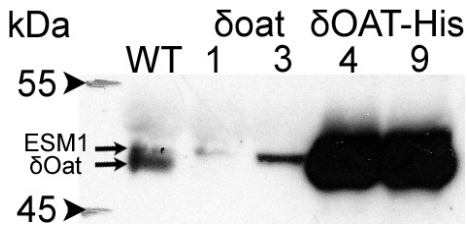

Figure 18: δOAT antiserum detects δOAT together with an unknown protein

Immunoblot showing the detection of δOAT in Arabidopsis wild type plants and δOAT-His overexpressing plants using the antiserum (1:1000) of a rabbit immunized with δOAT as antigen. The antiserum also detects a protein with a similar size as δOAT later identified as ESM1 (AT3G14210). ESM1 and δOAT are both detected in plant extracts of wild type plants, whereas only ESM1 is detected in *δoat* knockout plants (upper signal) (Funck *et al.*, 2008). The strong expression of δOAT-His in the overexpressing plants masks the weak signal of ESM1. δOAT and ESM1 are indicated by arrows.

In order to identify the unknown protein, a pull-down assay was performed applying total protein extract of *δoat* mutants to δOAT antibodies immobilized by cross-linking to Protein A sepharose beads. Antigens captured by the δOAT antibodies were eluted using potassium thiocyanate (KSCN), separated by SDS-PAGE and analysed by mass spectrometry (see also Chapter 4.11). The unknown protein of similar size to δOAT was identified as Epithiospecifier Modifier 1 (ESM1) with a sequence coverage of 40 % (Figure 19).

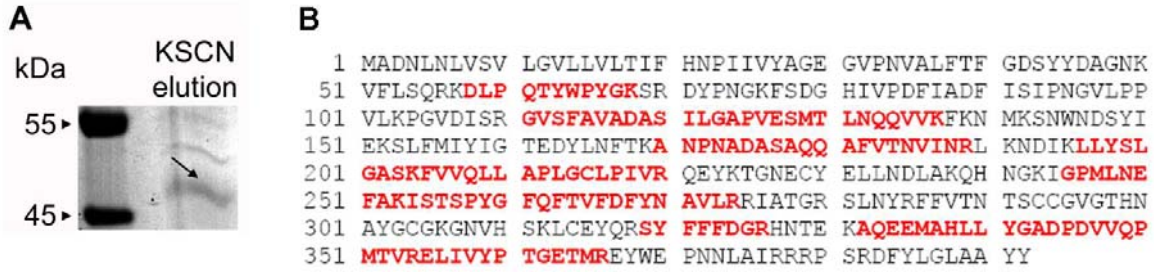

Figure 19: Pull-down with δOAT antiserum from δoat mutants (A) and identification of ESM1 by mass spectrometry (B)

A: Pull-down was performed by applying total soluble protein extract of *δoat* mutants to δOAT antibodies cross-linked to Protein A sepharose beads. Antigens detected by the antibodies were eluted using potassium thiocyanate (KSCN) and separated by SDS-PAGE. The signal in the size of δOAT (arrow) was cut out from the gel and analysed by mass spectrometry. B: peptides identified by mass spectrometry (red letters) in the primary sequence of ESM1 (sequence coverage: 40 %)

Since the cross-reaction of the δOAT antiserum with ESM1 probably impairs the interpretation of the results in a δOAT pull-down assay, recombinant ESM1 expressed in *E. coli* will be used in a first step for a negative absorption purification of the δOAT antiserum. In the following, the purified δOAT antiserum detecting only δOAT will be used for pull-down assays with protein extracts of Arabidopsis and subsequent identification of potential interaction partner of δOAT by mass spectrometry.

2.3.4. δOAT is not essential for utilization of nitrogen stored as arginine in seeds

δOAT is required for utilisation of arginine and ornithine as sole source of nitrogen and is therefore essential for arginine catabolism in Arabidopsis (Funck *et al.*, 2008). Since arginine is the most prominent amino acid for storage of nitrogen in seeds in different plant species (VanEtten *et al.*, 1963; King and Gifford, 1997) the physiological role of δOAT in arginine breakdown of Arabidopsis plants growing under nearly natural conditions is of great interest. Investigation of the elongation of hypocotyls of dark-grown seedlings under different nutrient conditions was used to assess the efficiency of storage mobilisation after germination in plants with different expression levels of δOAT. Neither with *δoat* mutants nor with δOAT overexpressing plants significant alterations in hypocotyl elongation in comparison to the wild type were detected (Figure 20). This indicates that δOAT-mediated release of nitrogen stored in arginine is not essential for expansion growth in very early seedling development.

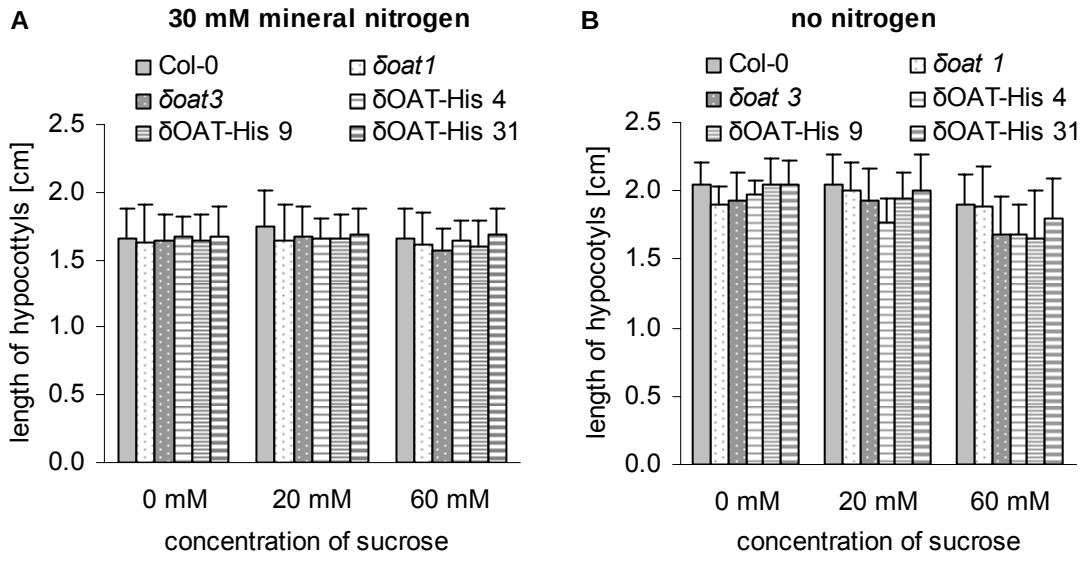

Figure 20: δOAT-mediated nitrogen recycling is not involved in hypocotyl elongation

δoat mutants and plants overexpressing His-tagged δOAT grown in darkness under different nutrient conditions for 14 days showed no significant differences in their hypocotyl length. Length of hypcotyls was measured by computational analysis using ImageJ. A: ½ MS complemented with 0 mM to 60 mM sucrose (no nitrogen depletion). B: ½ MS without nitrogen containing components (nitrogen depletion) complemented with 20 mM KCl and 0 mM to 60 mM sucrose. Error bars represent standard error of N = 30 plants. The experiments were repeated once with very similar results.

Since seedlings with knockout or overexpression of δOAT were unaffected with regards to hypocotyl elongation, seed yield of *δoat* mutants and δOAT overexpressing plants was analysed, investigating possible influences of δOAT on nitrogen remobilisation during seed development. δOAT-GFP overexpressing plants tend to produce a reduced total mass of seeds (Figure 21), which would match the hypothesis of a reduced ornithine pool available for arginine synthesis and its storage in seeds. Analysis of the individual seed weight of each knockout or overexpression line revealed that the reduced seed yield is mainly due to reduced amount of seeds per plant and not due to reduced seed size (data not shown). However, δOAT-GFP overexpressing plants showed also other phenotypical effects in comparison to plants overexpressing His-tagged δOAT (e.g. wrinkled leaves), indicating that the reduced seed weight per plant could also be due to overexpression of a mitochondrial GFP-fusion protein rather than increased δOAT-activity, which was very similar regardless of the overexpression construct (data not shown).

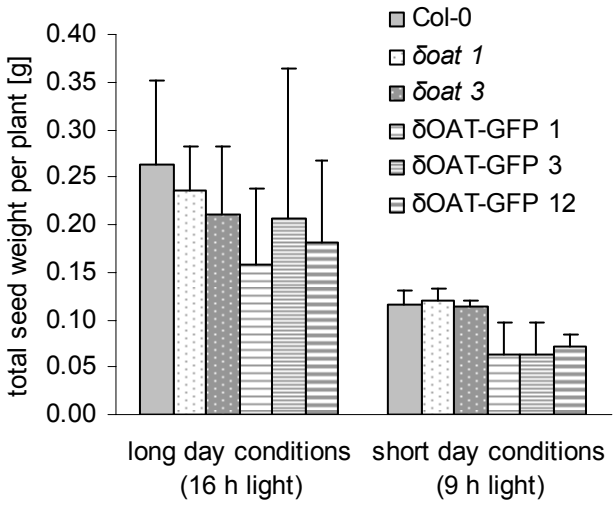

Figure 21: δOAT is not involved in regulation of seed yield

δoat mutants and GFP-tagged δOAT overexpressing plants grown on soil under long day (16 h light) or short day (9 h light) conditions until harvest (eight weeks) showed no significant differences in their total seed weight. Experiments were performed in three biological replicates each analysing eight plants of each line. Error bars represent standard error of n = 12 plants.

The findings that δOAT activity does not contribute significantly to expansion growth of seedlings or seed production raise the question in which other process nitrogen stored in form of arginine may be used. Seven-day-old *δoat* mutants seem to have a general growth problem because they showed highly significantly shorter roots and reduced leaf rosette diameters, independent of growth under control conditions or salt stress conditions (Figure 22, Luise Schönemann, personal communication). The rather non-essential role of δOAT and arginine catabolism in very early seedling development, suggests that other storage compounds are sufficient for germination and initial growth. When these resources are fully consumed at later stages of development, arginine recycling and therefore nitrogen recycling becomes limiting and growth is slowed down.

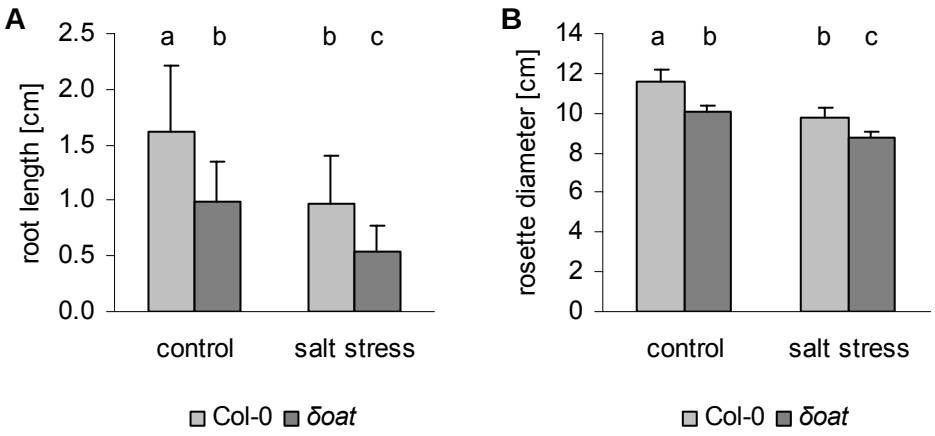

Figure 22: *δoat* mutants have shorter roots and reduced leaf rosette diameters

A: Root length of seven-day-old *δoat* mutants and wild type plants grown on ½ MS, 2 % (w/v) sucrose (control conditions) or on ½ MS, 2 % (w/v) sucrose, 50 mM NaCl (salt stress conditions). B: Five-week-old soil-grown *δoat*-mutants had smaller leaf rosettes than wild type plants under short day conditions (9 h light) both in the presence or absence of salt stress. Root length and leaf rosette diameters were determined from calibrated digital images. Error bars represent standard error of n = 80 plants (root length) and n = 40 plants (leaf rosette diameter) per treatment. a,b,c: Different letters indicate significant differences of statistical analysis using One-way-ANOVA ($p \leq 0.05$).

In addition, *δoat* knockouts accumulate ornithine produced from arginine by arginase which has to be recycled in arginine synthesis, because the exit route *via* δOAT to P5C followed by conversion to glutamate by P5CDH is blocked (Funck *et al.*, 2008) and the capacity for accumulation of ornithine may be limited in mitochondria. Arginine biosynthesis from ornithine involves two ATP-consuming steps: conversion of ornithine to citrulline by ornithine transcarbamylase (OTC) followed by the processing of citrulline to argininosuccinate by argininosuccinate synthase (ASSY) (Slocum, 2005). Forced to continuously cycle arginine and ornithine δ*oat* mutants constantly lose energy in arginine synthesis, energy actually needed for other cellular processes. As a consequence, *δoat* mutants may lack energy for growth resulting in shorter roots and reduced leaf rosette diameter.

As described, accumulation of ornithine in mitochondria is unfavourable in *δoat* mutants because of limited space in the mitochondrial matrix and the necessity of ornithine recycling in the energy-consuming arginine biosynthesis. A consequence of that could be the synthesis of polyamines from arginine as an alternative way to lower arginine levels. Increasing levels of the polyamines spermine and spermidine induce NO release

(Yamasaki and Cohen, 2006; Gupta *et al.*, 2011) and polyamine-mediated NO production is involved in root development and embryogenesis (Tun *et al.*, 2006). Assuming that polyamine synthesis remains as alternative sink for arginine conversion in *δoat* mutants, levels of NO could be increased to harmful concentrations with negative effects on root development and leaf rosette growth. Extremely high NO levels are discussed to interfere root and shoot development, beside impairment of photosynthetic electron transport, DNA damage and cell death (Qiao and Fan, 2008). Direct conversion of arginine to NO by NO synthase could be an additional sink for high arginine levels leading to the same effects as suggested for polyamines synthesis, although no NO synthase could be identified in Arabidopsis so far

Salt stress conditions reduced both root growth and leaf rosette sizes of wild type plants and *δoat* mutants (Figure 22). Since proline biosynthesis was suggested to contribute to root growth under salt stress conditions (Verslues and Sharp, 1999; Hong *et al.*, 2000), Roosens *et al.* (2002) hypothesized from higher root fresh weights of δOAT overexpressing plants that δOAT contributes directly to proline biosynthesis. In contrast to this hypothesis, the roots of *δoat* mutants are not affected excessively under salt stress in comparison to wild type plants (Figure 22). Wild type root growth was reduced by 40 % under salt stress, comparable to 45 % reduction of roots from *δoat* mutants. Leaf rosette sizes were reduced by 15 % in the wild type and 13 % in *δoat* mutants, also a very similar percental range. Taking this into account, it is unlikely that δOAT contributes directly to proline biosynthesis, because *δoat* mutants do not show increased sensitivity to salt stress in comparison to wild type plants. These results are in line with the conclusion of Funck *et al.* (2008), that δOAT is essential for arginine catabolism but not for proline biosynthesis, suggesting that the mitochondrial and cytosolic P5C pool are not linked by a P5C transporter as suggested by Phang (1985) and Miller *et al.* (2009).

It will be further investigated if the growth problem of young *δoat* mutants can be complemented with δOAT overexpression or saturating nitrogen fertilisation. For increased ornithine production and its potential effect on nitrogen recycling in Arabidopsis, arginase overexpressing plants will be crossed with *δoat* mutants and analysed physiologically in root and leaf rosette growth as well as general growth characteristics. Investigating the physiological role of δOAT will provide further details about its significance for arginine catabolism in Arabidopsis and for the process of recycling nitrogen stored in arginine.

3. Conclusion and Perspectives

Plants are often limited in growth by the availability of nutrients, and nitrogen is frequently the limiting factor for crop productivity. Therefore, nitrogenous fertilizers are extensively applied to improve agricultural yields. As the human population grows and the demand for agricultural products increases, it becomes important to understand the mechanisms of nitrogen acquisition, storage and recycling and their role in the metabolic and regulatory network of a plant cell. The aim of this work was to discover new aspects about the exact role of arginine and its catabolism in nitrogen recycling, focussing on the subcellular localization of the intracellular arginine transporters as well as on characterization of the arginine degradation enzymes arginase, δOAT and P5CDH.

The mitochondrial localization of two intracellular arginine transporters, BAC1 and BAC2, was predicted from their similarity to the mitochondrial carrier family (MCF) and from heterologous expression in yeast. In this work, the selective targeting of BAC1 and BAC2 to mitochondria was verified for the first time by the analysis of GFP fusion proteins. The exclusive mitochondrial localization led to the conclusion that BAC1 and BAC2 act only in the degradation pathway of arginine, whereas the export of newly synthesised arginine from chloroplasts has to be mediated by another transporter in the plastidial inner membrane, which is yet to be identified.

After arginine import into mitochondria by BAC1 and BAC2, it is processed by the arginase isoenzymes ARGAH1 and ARGAH2. Increasing the efficiency of substrate delivery and flux through a metabolic pathway requires quite often physical interaction of contributing enzymes. A cross-kingdom comparison of arginase sequences revealed a high level of conservation and allowed structural modelling of the Arabidopsis arginases. The structural model predicted trimers as basic unit for arginases and this study presents strong experimental evidence for homo- and hetero-oligomerisation of ARGAH1 and ARGAH2. The formation of mixed oligomers by ARGAH1 and ARGAH2 suggests that different compositions of homo- and hetero-oligomeric complexes display different arginase activities and could present a novel way to regulate arginase activity in different tissues or in response to environmental changes.

Substrate channelling in arginine catabolism can be decisive for the fate of the degradation products and therefore the possible connections between arginine and proline metabolism. The suggested formation of reversible enzyme complexes of δOAT and P5CDH that would prevent the release of potentially toxic P5C into the mitochondrial matrix could not be verified so far in this study. Support for the hypothesis of P5C channelling could be the observed homo-oligomerisation of P5CDH, which was experimentally shown for the first time in this study. It suggests two distinct, pH dependent oligomerisation complexes for P5CDH processing P5C from distinct pools, coming either from ProDH or δOAT and making the physical interaction of δOAT and P5CDH even more likely.

For further investigations of enzyme complexes involving δOAT, a specific antibody against δOAT is of great interest. In this work, a polyclonal antiserum against natively purified δOAT was raised in a rabbit and characterized with respect to sensitivity and specificity. δOAT-specific antibodies were enriched by affinity purification and will be further purified for application in a pull down assay of native δOAT-containing protein complexes from mitochondrial extracts, capturing potential interaction partners of δOAT.

Besides interaction characteristics and involvement in the metabolic network of the plant cell, the physiological role of arginine breakdown and especially of δOAT in Arabidopsis plants was of great interest. δOAT activity contributed not significantly to seed production or expansion growth of seedlings, suggesting a non-essential role of δOAT and arginine catabolism in very early seedling development. However, δ*oat* mutants were retarded in growth at later stages of development suggesting that nitrogen recycling from arginine becomes limiting, when other storage compounds, which are sufficient for germination and initial growth, are fully consumed. The growth-promoting effect of δOAT-mediated arginine catabolism may be essential for seed yield in natural conditions, although such an effect was not observed when plants were grown with saturating water and nutrients in the greenhouse.

Generation of double mutants with a complete knockout of arginine catabolising enzymes or combinations of overexpression and loss of function mutants resulting in accumulation of specific metabolites will help to determine the contribution of δOAT to an efficient recycling of nitrogen from arginine in plant cells. The

knowledge about essential intermediates and important developmental stages in nitrogen recycling of plants will help to understand the demands of developing plants, therefore enabling agriculture under conditions for optimal nitrogen recycling, which will reduce the effect of limited nitrogen for crop productivity.

4. Materials and Methods

4.1. Plant material and growth conditions

Arabidopsis (*Arabidopsis thaliana* (L.) Heynh. ecotype *Col-0*) and T-DNA insertion lines SALK_033541 (*oat1*) and SALK_106295 (*oat3*) were obtained from Dietmar Funck, Konstanz, Germany (Funck *et al.*, 2008). Plants were cultivated axenically in 9 cm Petri dishes on commercial MS medium (Duchefa, Haarlem, Netherlands) or self-made MS medium in which KNO_3 and NH_4NO_3 were replaced by 20 mM KCl (Murashige and Skoog, 1962). Media were supplemented with sucrose and nitrogen containing compounds as indicated for each experiment and solidified with 8 g/l purified agar (BD biosciences, San Jose, CA, USA) when appropriate. Seeds were surface sterilised by sequential treatment with 70 % (v/v) EtOH and 1 % (w/v) NaOCl/0.01 % (v/v) Triton-X-100 and vernalised for 24 h at 4 °C in 0.1 % (w/v) agarose. Plants were cultivated in a climatised room with short day (9 h) light period and a light intensity of 110 µmol photons$*s^{-1}*m^{-2}$ from mixed fluorescence tubes (Biolux and Fluora, Osram, Munich, Germany) at a constant temperature of 23°C. For seed production, plants were kept in a greenhouse with a light period of at least 16 h. *Nicotiana benthamiana* plants were cultivated on commercial gardening soil in the greenhouse under long day conditions.

4.2. BAC1-GFP and BAC2-GFP constructs and imaging

The open reading frames of *BAC1* and *BAC2* without stop codon were amplified by PCR from full-length ORF clones U82428 and U11604, respectively (ABRC, Columbus, OH, USA) (Yamada *et al.*, 2003). Sequences of PCR primers are given in Table 4. The resulting PCR fragments were purified and integrated into pENTR by directional TOPO cloning (life technologies, Carlsbad, CA, USA). Subsequently, the *BAC1* and *BAC2* cDNAs were transferred from pENTR to pEarleyGate103 (CD3-685, ABRC) or pGWB5 (Nakagawa *et al.*, 2007) by LR-recombination (life technologies), yielding *BAC1-GFP* or *BAC2-GFP* fusion genes under control of the 35S cauliflower mosaic virus promoter. Both plant transformation vectors yielded the same results. Transformation of Arabidopsis plants by floral dip was performed according to Clough and Bent (1998). Transformants were selected on plates

containing ½ MS media supplemented with 2 % sucrose, 150 µg/ml Cefotaxim, 150 µg/ml Ticarcilin and 10 µg/ml BASTA® (Bayer AG, Leverkusen, Germany) for pEarlyGate103 constructs and 50 µg/ml Kanamycin for pGWB5 constructs.

Protoplasts from leaves of BAC1-GFP or BAC2-GFP expressing plants were obtained by overnight incubation with cellulase and macerase (Serva, Heidelberg, Germany) in ½ MS media/0.45 M sorbitol, stained with MitoTracker Orange (life technologies). Protoplasts were viewed with a 40 x oil immersion lens on a Zeiss LSM 510 Meta confocal microscope (Zeiss, Oberkochen, Germany). GFP, MitoTracker and chlorophyll fluorescence signals were sequentially captured with the Meta detector of the confocal microscope (GFP: 497–550 nm, MitoTracker orange: 572-615 nm, chlorophyll: 657–690 nm). False colouring of images and linear unmixing (Chapter 4.3) was performed using ZEN software (Zeiss, Oberkochen, Germany). Overlay of the images was done with ImageJ and Adobe Photoshop.

For *in vivo* fluorescence microscopic imaging of leaf epidermis cells, leafs infiltrated with 0.1 M KCl/0.01 % Silwet were viewed on an Olympus BX51 epifluorescence microscope equipped with an AxioCam MRm digital camera system (Carl Zeiss Microscopy GmbH, Jena, Germany). Chlorophyll autofluorescence and GFP fluorescence of the cells were dissected using the filter sets U-MWSG2 (Olympus) and 41020 (Chroma Technology Corp, Rockingham, VT, USA), respectively. False colouring and overlay of images were performed using AxioVision software (Zeiss, Oberkochen, Germany).

4.3. Linear unmixing

Due to ambiguous localization results from images with overlays of Mitotraker, GFP and chlorophyll autofluorescence subcellular localization was studied by spectral analysis using the linear unmixing tool of the ZEN software.

Fluorescence emission was collected in a lambda stack from 502 to 641 nm with 10-11 nm per channel and the spectral distribution of a defined region was used as reference spectrum for linear unmixing. The GFP spectrum was recorded from a plant expressing a P5CR-GFP fusion construct in the cytosol (Figure 23) (Funck *et*

al., 2012). Nontransformed Arabidopsis *Col-0* (wild type) plants were used for reference spectra of chlorophyll and cell wall autofluorescence. The chlorophyll lambda stack was collected from a *Col-0* leaf mesophyll chloroplast. GFP and cell wall spectra were recorded from a root cell image, in order to obtain signals that are not influenced by chlorophyll autofluorescence.

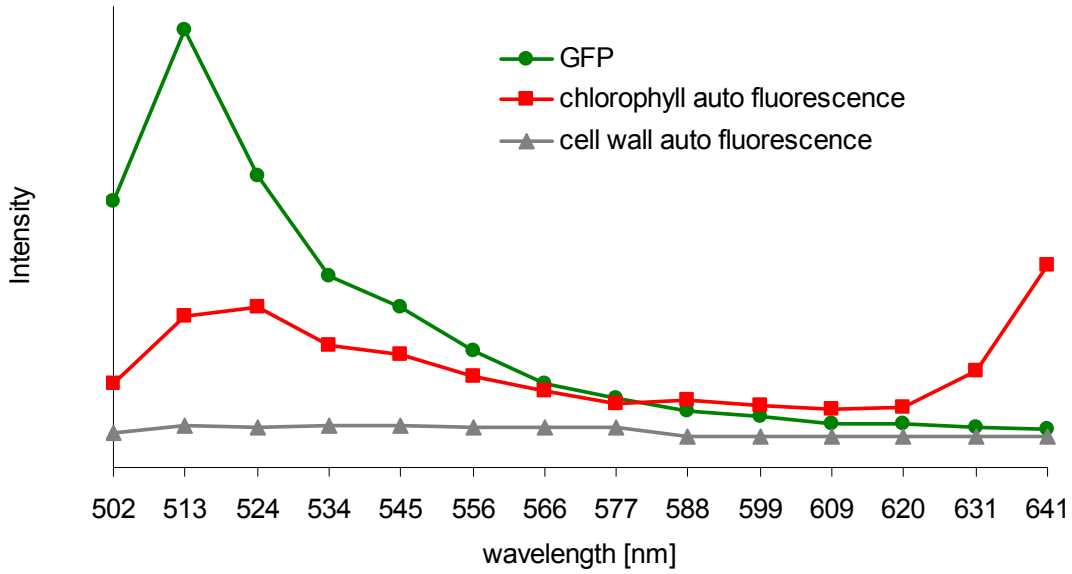

Figure 23: Reference spectra for GFP, chlorophyll auto fluorescence and cell wall auto fluorescence

Intensity of the cell wall fluorescence spectrum averaged 1/5 of the maximum GFP or 1/3 of the maximum chlorophyll spectral intensities and was subtracted from spectral images as background spectrum (typical image in Figure 24 A, cell wall autofluorescence image of BAC1-GFP (Figure 8, D, E, F)).

The linear unmixing tool of the ZEN software presents a residual image after analysis and assignment of the spectral data. This reveals semi-quantitative information about the precision of the spectral dissection. Spectral signals that do not match those in the reference spectra are considered residual and are not assigned. Major reasons for this are saturated pixels, high background levels or fluorescence from sources that were not represented in the reference spectra. Very low intensity of the residual signal (typical image in Figure 24 B, residual image of BAC1-GFP (Figure 8, D, E, F)) demonstrated that nearly all fluorescence signals

could be assigned to either GFP, chlorophyll or cell wall and verifies the reliability of spectral unmixing.

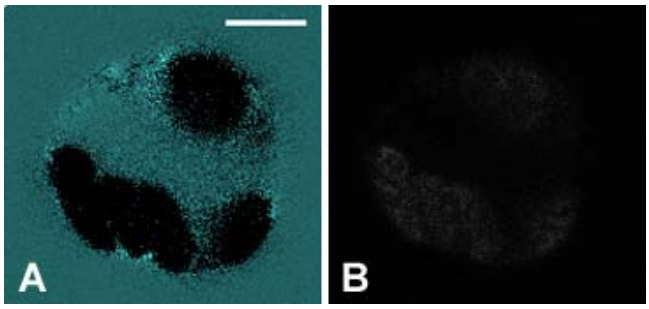

Figure 24: Example of a cell wall auto fluorescence and a residual image after linear unmixing

A: Cell wall autofluorescence image of BAC1-GFP (Figure 8, D, E, F), was subtracted from spectral images as background spectrum. Bar: 5 µm, B: Residual image of BAC1-GFP (Figure 8, D, E, F). Very low intensity of the residual signal demonstrates that nearly all fluorescence signals could be assigned to GFP, chlorophyll or cell wall and verifies the reliability of spectral unmixing.

4.4. Alignments and Modelling of ARGAH1 and ARGAH2

Alignments of arginase sequences were performed using BioEdit (http://www.mbio.ncsu.edu/BioEdit/bioedit.html) and its ClustalW tool (Thompson *et al.*, 1994) using Phylip4.0 as output format. All sequences used for the alignments were identified with the basic local alignment search tool (BLAST) for protein sequences from NCBI (http://www.ncbi.nlm.nih.gov/). Protein hits annotated as arginase were retrieved (Table 3) and used for the alignment.

Table 3: Arginase sequences used for ClustalW alignment

Organism	Accession number	Name of Protein
Arabidopsis thaliana	gi|1168493	Argah1
Arabidopsis thaliana	gi|11131457	Argah2
Medicago truncatula	gi|357469765	arginase
Oryza sativa Japonica Group	gi|115456826	Os04g0106300
Solanum lycopersicum	gi|350538013	arginase 1
Solanum lycopersicum	gi|350538867	arginase 2
Synechocystis sp. PCC 6803	gi|16329302	arginase
Homo sapiens	gi|346986435	arginase-1

Homo sapiens	gi|4502215	arginase-2
Rattus norvegicus	gi|149032924	arginase 1
Rattus norvegicus	gi|9506399	arginase-2
Saccharomyces cerevisiae S288c	gi|6325146	arginase

For structure modelling the Protein Homology/analogY Recognition Engine V 2.0 (Phyre2, http://www.sbg.bio.ic.ac.uk/phyre2/html/page.cgi?id=index) (Kelley and Sternberg, 2009) was fed with protein sequences of ARGAH1 and ARGAH2 lacking the predicted mitochondrial transit peptide (ARGAH1: first 18 amino acids, ARGAH2: first 35 amino acids, prediction from MitoProtII: http://ihg.gsf.de/ihg/mitoprot.html) (Claros and Vincens, 1996). Modelled structures and the crystal structure of rat arginase 1 (PBD ID: 1ZPG) (Colleluori *et al.*, 2005) were visualised with Jmol (http://www.jmol.org/).

4.5. PCR-Primers

General molecular biological procedures were conducted according to Sambrook *et al.* (1989). Sequences of primers used in this study are given in Table 4.

Table 4: PCR-Primers used in this study

Name	Sequence (5'>3')	Used for
AtmBAC1-Entry-f	caccATGGGAGAGAGTAAGACGACGAC	BAC1 cloning
AtmBAC1ns-r	GTCACGTTTGATTCCCAAC	
AtmBAC2-Entry-f	caccATGGATTTCTGGCCGGAGTTTATG	BAC2 cloning
AtmBAC2ns-r	ATCTCCTGTGACAATATCTGGGGA	
Oat-Entr-f	caccATGGCAGCCACCACGAGACG	*Oat* cloning
Oat-s-r	CaaaccggtTCAAGCATAGAG	*Oat* cloning with stop codon
Oat-ns-r	cGCATAGAGGTTTCTTCCACAG	*Oat* cloning without stop codon
Oat-48-Bam-f	CCggatccatgTCTACCGCCGGAGTGCGGCGGAG	*Oat* cloning for overexpression in *E. coli*
OatflBam-r	ctGGATCCaaaccggtTCAAGCATAGAG	*Oat* cloning for overexpression in *E. coli*
Oat-His-s-r	gactaATGGTGATGGTGATGATGcGCATAGAGGTTTCTTC	*Oat*-His cloning

Name	Sequence (5'>3')	Used for
DL1-Entry-Koz-f	CACCaCAatgGTtagagtttttgcgag	*P5CDH* cloning
DL1-XhoI-r	cacTcGaGttCTAAGTAGATGGAGGAAGTTC	*P5CDH* cloning with stop codon
Oat-N48-Entr-f	caccTCTACCGCCGGAGTGCGGCGGAG	*Oat*-N48 cloning
His-Oat-N48-Entr-f	caccACTATGAGAGGATCGCATCAC	His-*Oat*-N48 cloning
Oat-N102-Entr-f	caccTCTCCTCCGTCTTCTTCTC	*Oat*-N102 cloning
Argah1-Entr-f	caccATGTCGAGGATTATTG	*Argah1* and *Argah2* cloning
Argah2-Entr-f	caccATGTGGAAGATTGGG	
Argah1-28-Ef	caccATCGAGAAAGGGCAAAATCG	
Argah2-30-Ef	caccGTCGAGACAGGGCAGAACC	
Argah1s-r	gaggcctcaTTTCGAGATTTTC	
Arg1ns-r	TTTCGAGATTTTCGCAGCTAATTC	
Argah2s-r	ccatttaaattcaTTTTGACATTTTTGC	
Arg2ns-r	TTTTGACATTTTTGCGGCTAGCTC	
Arg1STREPIIc-r	ctctaTTTTTCGAACTGCGGGTGGCTCCAtccacTTTCGAGATTTTCGCAGCTAATTC	
Arg2STREPIIc-r	ctctaTTTTTCGAACTGCGGGTGGCTCCAtccacTTTTGACATTTTTGCGGCTAGCTC	
P5CDH-N39-Entr-f	caccTCTCTCTGTGACAAATCATCCAC	*P5CDH*-N39 cloning
DL1oMT24-f	caccTCTTTGACTCTCTCCAGATTG	*P5CDH*-N75 cloning
ProDH-entry-Koz-f	CACCataATGGCAACCCGTCTTCTC	*mTP-ProDH1* cloning
ProDH1-probe-r	ATGGTCATAAAACGTACTTTTCAC	

4.6. Western blot analysis of protein expression

Proteins of Arabidopsis and tobacco for SDS-PAGE and western blot analysis were extracted as described in Kupper *et al.* (2008). Total proteins from yeast were extracted from a culture with OD_{600nm} = 2 (grown over night from a 1:1000 diluted pre-culture at 30 °C). The cells were centrifuged at 4000 x g for 20 min at 4 °C. The cell pellet was washed in 500 ml cold water and pelleted again by centrifugation. Cells were resuspended in cold water and transferred to a 50 ml tube and

centrifuged again for 15 min. The supernatant was discarded, the pellet was frozen in liquid nitrogen and stored at -20 °C until protein extraction. For protein extraction the pellet was thawed in extraction buffer (10 mM K-HEPES, pH7,9; 10 mM KCl; 1.5 mM $MgCl_2$; 0.5 mM DTT; 2 x Roche Protease Inhibitors) and passed through the French press twice (max. pressure 8 MPa). The lysate was complemented with 0.2 M KCl (final concentration) and cell debris was separated by ultracentrifugation (33000 x g, 30 min, 4 °C). The supernatant was transferred to new centrifuge tube and the non-lipidic phase was separated again by ultracentrifugation (88000 x g, 30 min, 4 °C). The lower non-lipidic phase was centrifuged again for 1 h. The final soluble protein fraction was saved and used for Western blot analysis (Towbin *et al.*, 1979). Five to 10 µg total protein extract were loaded onto 7-12 % SDS gels (Laemmli, 1970) prior to their transfer to PVDF western blotting membranes (Roche, Mannheim, Germany) using a semi-dry blotting system (Biometra, Göttingen, Germany). Primary antibodies and conjugates are listed in Table 5. Blots were developed using horseradish peroxidase-coupled IgG (Sigma-Aldrich, Hamburg, Germany) followed by chemiluminescence detection (ECL plus, GE healtcare, Amersham Bioscinece, Uppsala, Sweden).

Table 5: Antibodies and conjugates

Name	Company/ Publication	Product Number	Organism	Dilution
anti-GAL4 DNA-BD	Sigma-Aldrich, Hamburg, Germany	G 3042	rabbit	as recommended by supplier
anti-GAL4 AD	Sigma-Aldrich, Hamburg, Germany	G 9293	rabbit	as recommended by supplier
anti-arginase serum	Todd and Gifford (2002)	-	rabbit	1:5000
anti-His HRP conjugate	Qiagen, Hilden, Germany	34460	mouse	as recommended by supplier
Strep-Tactin HRP conjugate	iba, Göttingen, Germany	2-1502-000	-	as recommended by supplier

4.7. Plasmid construction for Yeast two-hybrid assays

The open reading frame of Arabidopsis *Ornithine-δ-aminotransferase* (*δOat*, AT5G46180) was amplified by PCR from EST clone H4E5 (GenBankAccession W43737, ABRC, Ohio). The resulting PCR fragments were purified and integrated into pENTR by directional TOPO cloning (life technologies, Carlsbad, CA, USA), resulting in the plasmids pEntrOat-s and pEntrOat-ns. N-terminally truncated versions excluding the predicted mitochondrial transit peptides as well as plasmids containing full length and truncated versions of *Argah1*, *Argah2*, *ProDH* and *P5CDH* were generated in the same way (Table 6). Subsequently, the respective cDNAs were transferred from pENTR to Gateway®-modified (Schuhmann *et al.*, 2011) pAD-GAL4 2.1 (Stratagene, introducing the GAL4 activation domain) or pBD-GAL4 Cam (Stratagene, introducing the GAL4 DNA binding domain) by LR-recombination (life technologies).

Table 6: pENTR vectors for LR-recombination with Y2H pAD-GAL4/pBD-GAL4 vectors

Name of gene	Locus	Clone/vector used for amplification	pENTR-Name	Primer (for sequence see Table 4)
δOat	AT5G46180	EST clone H4E5	pEntrOat-s	Oat-Entr-f + Oat-s-r
(GenBank Accession W43737, ABRC, Ohio)			pEntrOat-N48	Oat-N48-Entr-f + Oat-s-r
			pEntrOat-N102	Oat-N102-Entr-f + Oat-s-r
Argah1	AT4G08900	U13642	pEntrArgah1-s	Argah1-Entr-f + Argah1-s-r
(GenBank Accession AY061914, ABRC, Ohio)			pEntrArgah1-ns	Argah1-Entr-f + Argah1-ns-r
Argah2	AT4G08870	C105130	pEntrArgah2-s	Argah2-Entr-f + Argah2-s-r
(GenBank Accession BT003815, ABRC, Ohio)			pEntrArgah2-ns	Argah2-Entr-f + Argah2-ns-r
ProDH1	AT3G30775		pEntr-Pdh1-s	(Funck *et al.*, 2010)
P5CDH	AT5G62530	pYES-DL1-HX1-3-1	pEntrP5CDH	DL1-Entry-Koz-f + DL1-XhoI-r
		(Deuschle *et al.*, 2001)	pEntrP5CDH-N39	P5CDH-N39-Entr-f + DL1-XhoI-r
			pEntrP5CDH-N75	DL1oMT24-f + DL1-XhoI-r

All plasmids were analyzed by PCR, restriction analysis and sequencing (GATC Biotech. AG, Germany) for orientation and integrity of the insert.

4.8. Yeast two-hybrid assay (Y2H)

For all Y2H assays the vectors pBD-Gal4 Cam as bait vector and pAD-Gal4 2.1 as prey vector from the GAL4 Phagemid Vector Kit (Stratagene, Germany) were used. See 4.4 for details of cloning of the respective plasmids. pBD-WT and pAD-WT (Stratagene, Germany) are both coding for fragment C of the lambda cl repressor and served as positive interaction control plasmids. pAD-WT and pLamin C (Stratagene, Germany), coding for human lamin C, were used as negative interaction control plasmids. *S. cerevisiae* strain YRG-2 (genotype: Mat**a** *ura3-52 his3-200 ade2-101 lys2-801 trp1-901 leur2-3 112 gal4-542 gal80-538* LYS2::UAS$_{GAL1}$-TATA$_{GAL1}$-HIS3 URA3::$_{UASGAL4\ 17mers(x3)}$-TATA$_{CYC1}$-*lacZ*; Note: The LYS2 gene in this strain is non-functional, Stratagene, Germany) was used for all Y2H assays. For composition of media see the manual of the GAL4 Phagemid Vector Kit (Stratagene, Germany). Yeast transformation by the lithium acetate method was performed as recommended by Gietz and Woods (2002). For *HIS3* reporter gene assays, candidate clones were cultured in liquid Synthetic Complete dropout (SC) media lacking Leucine, Uracil and Tryptophan overnight, pelleted and resuspended to an OD_{600} of 1.0. 50 µL of the suspension and two dilutions (1:10 and 1:100) were dropped on solid SC medium lacking Leucine, Uracil and Tryptophan (growth control) or Histidine, Leucine, Uracil and Tryptophan (reporter gene assay), respectively. Plates were grown for 2-3 days at 30° C.

To screen for alternative interaction partners of Oat, pBDOat-fl was used as bait plasmid and the Horwitz and Ma Two-Hybrid Library (Stock: CD4-30, ABRC, Ohio) (Fan *et al.*, 1997) as prey library. Candidate colonies growing on SC agar plates lacking Histidine were restreaked on the same media and incubated for three days at 30 °C. Individual colonies were used to inoculate liquid SC media lacking Leucine, Uracil and Tryptophan, grown overnight and the *HIS3* reporter gene assay was repeated as described above for verifying the interaction. If complementation of the *HIS*-auxotrophy was observed again, plasmid DNA from three independent colonies was prepared according to Ausubel *et al.* (1991) and

analysis by restriction with HindIII for the presence of a single plasmid. Plasmids were re-introduced into YRG-2 cells together with empty pBD-Gal4 Cam (auto-activation control) or pBD-Oat-fl (interaction with Oat-fl) and *HIS3* reporter gene activation was assayed as described above. Plasmids that did not show self induced activation but reporter gene activation with pBD-Oat-fl were sequenced (GATC Biotech. AG, Germany).

4.9. Co-expression and co-purification of ARGAH1 and ARGAH2

Co-expression and co-purification of Arabidopsis *Arginase1* and *Arginase2* (*Argah1,* AT4G08900*; Argah2*, AT4G08870) was performed using the truncated variants *Argah1*-N28 (lacking the first 28 amino acids) and *Argah2*-N30 (lacking the first 30 amino acids). For Strep-tagged proteins *Argah1*-N28 and *Argah2*-N30 were amplified by PCR from pEntrArgah1-ns or pEntrArgah2-ns (Chapter 4.7), respectively, using the primers Argah1-28-Ef and Arg1STREPIIc-r or Argah2-30-Ef and Arg2STREPIIc-r. The resulting PCR fragments were purified and ligated into *Xba*I/*Nhe*I-linearized pET24a after fill-in of the 5' overhangs with the Klenow fragment of *E. coli* DNA polymerase, resulting in the plasmids pET24a-Argah1-N28-Strep and pET24a-Argah2-N30-Strep. For His-tagged proteins *Argah1*-N28 and *Argah2*-N30 were amplified by PCR from pEntrArgah1-s or pEntrArgah2-s (Chapter 4.7), respectively, using the primers Argah1-28-Ef and Arg1ns-r or Argah2-30-Ef and Arg2ns-r. The resulting PCR fragments were purified and integrated into pET151 by directional TOPO cloning (life technologies), resulting in the plasmids pET151-His-Argah1-N28 and pET151-His-Argah2-N30. All plasmids were analyzed by PCR, restriction analysis and sequencing (GATC Biotech. AG, Germany) for orientation and integrity of the insert. Subsequently, *E. coli* BL21* was transformed with the expression constructs for Strep-tagged proteins. The resulting expression clones were again transformed with the His-tagged counterpart arginase isoform, resulting in clones expressing both arginase isoforms, Strep- and His-tagged, simultaneously.

For co-expression a culture was inoculated at OD_{600nm} = 0.4 with a pre-culture of *E. coli* BL21* pET24a-Argah1-N28-Strep/pET151-His-Argah2-N30. The expression culture was incubated at 17 °C for 6 h or until an OD_{600nm} = 0.6 was reached,

expression was induced with 0.3 mM IPTG and the cells were cultivated over night at 17 °C for protein expression. For harvesting cells were centrifuged for 10 min at 6000 x g, washed once with distilled water and transferred to 50 ml tubes. After centrifugation for 10 min at 6000 x g, cell pellets were frozen in liquid nitrogen and stored at -20 °C until protein extraction. For protein extraction cells were thawed on ice and resuspended in lysis buffer (50 mM Na-HEPES, pH7.5; 100 mM NaCl; 5 mM $MgCl_2$; 1 mM $MnCl_2$; 25 mM Imidazole). Cell lysis was performed by 6 x sonication for 10 sec each, cell debris was pelleted by centrifugation at 10000 x g for 20 min and the supernatant was filtered (pore size 0,2 µm). The lysate was injected in an ÄKTA purifier system and purification was performed with 25 mM imidazole for binding (binding buffer: 50 mM Na-HEPES, pH7,5; 100 mM NaCl; 5 mM $MgCl_2$; 25 mM Imidazole) and an imidazole gradient to 500 mM imidazole (elution buffer: 50 mM Na-HEPES, pH7,5; 100 mM NaCl; 5 mM $MgCl_2$; 500 mM Imidazole). Elution fractions containing protein were frozen at -20 C. For western blot analysis proteins were precipitated by adding acetone. Protein pellets were dried and dissolved in 1 x loading buffer (2 % Lithium-dodecyl-sulfate (LDS), 50 mM Tris-HCl, pH8, 1 % dithiothreitol (DTT), 0.02 % bromphenol blue, 10 % glycerol). SDS-PAGE and western blot analysis were performed as described above (Chapter 4.6).

4.10. Vector and plasmid construction for bimolecular fluorescence complementation (BiFC) assays and tobacco infiltration

For cloning of Gateway®-compatible BiFC vectors for agrobacterium-mediated transformation of Arabidopsis or *N. benthamiana* pSAT-vectors (Citovsky *et al.* (2006), pSAT4A-DEST-nEYFP-N, pSAT4-DEST-nYFP-C, pSAT5A-DEST-cEYFP-N, pSAT5-DEST-cEYFP-C; (Stock numbers CD3-1083, CD3-1092, CD3-1096 and CD3-1097, respectively; ABRC, Columbus, OH, USA) were digested using rare cutters (pSAT4-vectors: I-*Sce*I, pSAT5-vectors: I-*Ceu*I), excising the split-YFP Gateway® cassette. After fill in of 5' overhangs and purification, the split-YFP Gateway® cassettes were ligated into the *Sma*I linearised and dephosphorylated pPZP212 (plant resistance: kanamycin) or pPZP312 vectors (plant resistance: BASTA®) (Hajdukiewicz *et al.*, 1994), respectively, resulting in the vectors pPZP212-c/nYFP-C (N-terminal YFP), pPZP212-c/nYFP-N (C-terminal YFP) or

pPZP312-c/nYFP-C (N-terminal YFP), pPZP312-c/nYFP-N (C-terminal YFP) (Figure 25).

Subsequently, the *Arginase1* or *Arginase2* cDNA with out stop codon were transferred from pENTR (Chapter 4.7) to pPZP212-c/nYFP-N (plant resistance: kanamycin, c-terminal YFP) by LR-recombination (life technologies), resulting in the plasmids pPZP212-ARGAH1ns-cYFP, pPZP212-ARGAH1ns-nYFP, pPZP212-ARGAH2ns-cYFP and pPZP212-ARGAHns-nYFP. All plasmids were analyzed by PCR and restriction analysis for orientation of the insert.

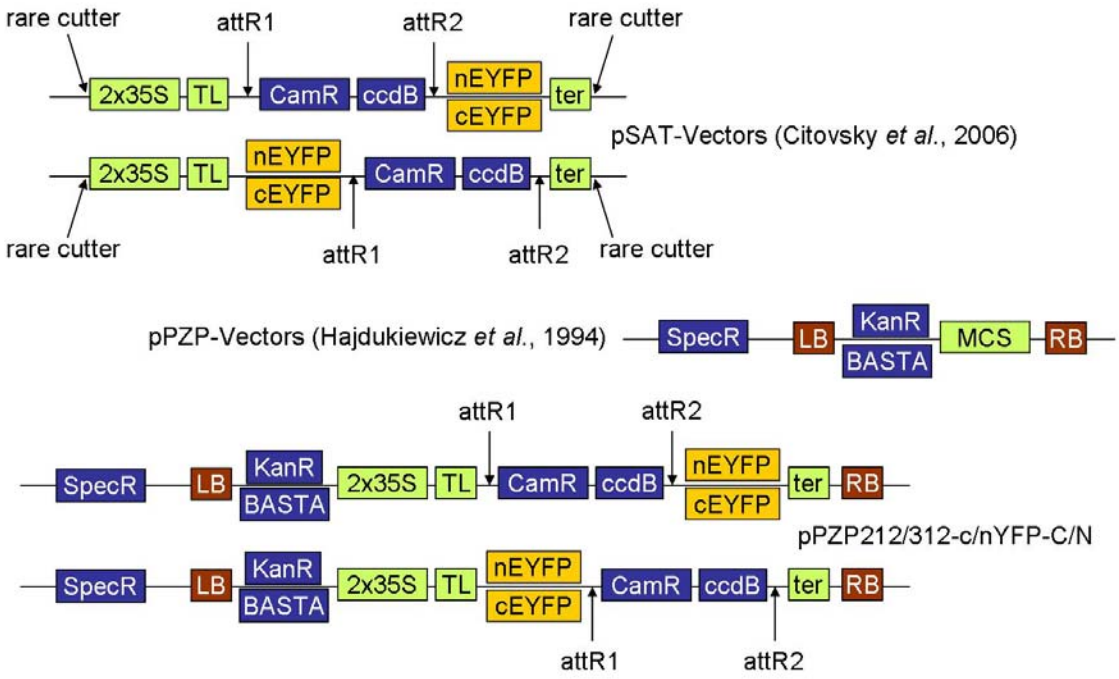

Figure 25: Vectors for BiFC plasmid construction

For construction of Gateway® compatible BiFC vectors for agrobacteria mediated transformation, expression cassettes from pSAT-vectors were inserted into the T-DNA region of pPZP-vectors. 2x35S: tandem CaMV 35S promoter; TL: TEV translation leader; ter: CaMV 35S poly(A) transcriptional terminator; nEYFP and cEYFP: the N-terminal and C-terminal fragments of EYFP; CamR: chloramphenicol resistance; ccdB: ccdB toxin gene; SpecR: spectinomycin resistance; LB: left border; RB: right border; KanR: kanamycin resistance; BASTA: Basta® resistance; MCS: multiple cloning site; attR1/attR2: Gateway® recombination sites

For investigation of the efficiency of co-transformation of tobacco cells with agrobacteria cultures harbouring two different fusion constructs, the mitochondrial transit peptide (mTP) of proline deyhdrogenase 1 (ProDH1) was tagged either GFP

or CFP. Therefore, the mitochondrial transit peptide of ProDH1 was amplified by PCR from pEntr-ProDH1 (Funck *et al.*, 2010) using the primers ProDH-entry-Koz-f and ProDH-probe-r (Table 4). The resulting PCR fragments were purified and integrated into pENTR by directional TOPO cloning (life technologies, Carlsbad, CA, USA), resulting in the plasmid pEntr-mTP-ProDH. Subsequently, the *mTP-Pdh* cDNA was transferred from pENTR to pEarleyGate103 (CD3-685, ABRC) or pEarleyGate102 (CD3-684, ABRC) by LR-recombination (life technologies), yielding *mTP-ProDH-GFP* or *mTP-ProDH-CFP* fusion genes under control of the CaMV 35S promoter.

A. tumefaciens strains LBA4404 and GV3101 were used for transient transformation of tobacco. All split-YFP plasmids or plasmids containing *mTP-ProDH-GFP* or *-CFP* genes were introduced into competent *A. tumefaciens* cells by heat shock transformation. Cells of PCR positive clones were grown to stationary phase and were diluted to an OD_{600} of 0.8 with AS medium (10 mM MES/KOH, pH5.6; 10 mM $MgCl_2$; 150 mM acetosyringon). For co-expression agrobacteria, harbouring a fusion construct containing the C-terminal fragment of YFP or GFP-tagged mTP-ProDH, were mixed 1:1 with agrobacteria expressing a fusion protein containing the N-terminal fragment of YFP or CFP-tagged mTP-ProDH and leaves of 4-6 week old *N. benthamiana* plants were infiltrated. After two days of infection, leave peaces were vacuum infiltrated through the stomates of the lower epidermis with a 1 ml syringe. Two days after of infiltration, leaf peaces were vacuum infiltrated with 0.1 M KCl/0,01 % (v/v) Silwet-Gold and analysed by epifluorescence microscopy (Chapter 4.2, filter sets: U-MWSG2 (Olympus) for chlorophyll autofluorescence, U-MF2 41007 (Olympus) for YFP fluorescence, U-MF2 41020 (Olympus) for GFP fluorescence, U-MF2 31045 (Olympus) for CFP fluorescence). For SDS-PAGE and western blot analysis proteins were extracted as described in (Kupper *et al.*, 2008).

4.11. δOAT antibody production and verification of antibody specificity

Polyclonal antibodies were raised against the recombinant δOAT from *A. thaliana* expressed in *E. coli*. The full-length δOAT cDNA without mitochondrial transit peptide (first 48 amino acids) was amplified using the primers Oat-48-Bam-f and

OatflBam-r (Table 4) from EST clone H4E5 and integrated into the *Stu*I site of the vector pCRblunt by ligation. The δOAT cDNA was excised with *BamH*I and ligated into the unique BamHI site of the vector pQE-30 (Qiagen, Hilden, Germany) for bacterial expression. Clones with the correct orientation of the δOat-cDNA were identified by PCR and restriction analysis, absence of PCR errors was verified by sequencing (GATC). The δOAT protein was expressed in *E. coli* SG13009 (Qiagen, Hilden, Germany) as fusion protein with an N-terminal attached His-tag (6 x His) according to the manufacturer's protocol (The QIAexpressionist, 2003). Cells were grown to an OD_{600} of 0.4 at 37 °C and expression of the recombinant protein was induced by adding isopropyl ß-D-1-thiogalactopyranoside (IPTG) to a final concentration of 0.4 mM. Five hours after induction cells were harvested and frozen in liquid nitrogen. For protein preparation cells were thawed and pellets were resuspended in lysis buffer (50 mM NaH_2PO_4, pH 8, 300 mM NaCl, 10 mM Imidazole, 0.15 mM Pyridoxal phosphate) and incubated with 1 mg/ml Lysozym for 30 min on ice, prior to cell disruption by sonication (6 x 10 sec). Cell debris were separated by centrifugation (10,000 x g, 30 min, 4 °C) and recombinant δOAT was purified under native conditions from the supernatant by affinity chromatography on Ni-NTA-agarose columns (1 ml HisTrap FF, GE Healthcare, Little Chalfont, UK) and eluted from the column with elution buffer (50 mM NaH_2PO_4, pH 8, 300 mM NaCl, 500 mM Imidazole). Eluted fractions containing δOAT were pooled and desalted to low salt buffer (50 mM NaH_2PO_4, pH 8, 25 mM NaCl) using a desalting column (HiTrap G25-5ml, GE Healthcare, Little Chalfont, UK). Desalted δOAT was purified in a polishing step by ion exchange chromatography on a quartenary amine minicolumn (HiTrap Q, 1ml, GE Healthcare, Little Chalfont, UK). δOAT was eluted from the column by high salt buffer (50 mM NaH_2PO_4, pH 8, 500 mM NaCl) and δOAT containing fraction were pooled, frozen in liquid nitrogen and stored at -80 °C. Purity of the δOAT protein was confirmed by separation on SDS-PAGE and Western blot. The purified protein was used to raise a polyclonal antibody in rabbit (laboratory Animal Facility, Konstanz University, Germany).

The specificity of the δOAT antiserum was tested using protein extracts of Col-0, δ*oat1*, δ*oat3*, δOAT-His4 and δOAT-His9 (Chapter 4.12) plants. Western blots revealed a strong reaction with δOAT but also reaction with several other proteins, of which on had a very similar molecular weight as δOAT. Hence, a purification of the antiserum was necessary, using P5CR, expressed in pET151 in *E. coli* (Funck

et al., 2012), for negative adsorption and affinity chromatography purified δOAT for positive adsorption on sepharose columns. After concentration of the δOAT antibodies by negative and positive adsorption, the unspecific signal was still detected. Identification of the unknown protein was performed using immunoprecipitation and mass spectrometry. For immunoprecipitation δOAT antibodies were cross-linked using dimethyl pimelimidate (DMP) to EZview Protein A Sepharose beads (Sigma-Aldrich, St. Louis, MO, USA). Cross-linked antibodies were incubated 5 x 2 h with a protein extract from δ*oat3* mutant plants and bound proteins were eluted using 5 M potassium thiocyanate (KSCN). The eluate was separated by SDS-PAGE, stained with Coomassie brilliant blue and a protein band with the expected molecular weight was cut and analysed by mass spectrometry (Proteomics Facility, Konstanz University, Germany).

4.12. δOAT-GFP and δOAT-His constructs

δOAT-GFP overexpressing plants were obtained from Dietmar Funck (Funck *et al.*, 2008). For δOAT-His constructs the open reading frame of Arabidopsis *Ornithine-δ-aminotransferase* (*δOat*, AT5G46180) was amplified by PCR from EST clone H4E5 (GenBankAccession W43737, ABRC, Ohio) using the primers Oat-Entr-f and Oat-His-s-r (Table 4). The resulting PCR fragments were purified and integrated into pENTR by directional TOPO cloning (life technologies), resulting in the plasmid pEntrOat-His. Subsequently, the *Oat*-His cDNA from HaeII linearised pEntrOat-His was transferred to pEG100 (Earley *et al.*, 2006) by LR-recombination (life technologies), resulting in the plasmid pEG100-Oat-His. *Agrobacterium tumefaciens* strain LBA4404 was used for floral dip transformation of Arabidopsis (Clough and Bent, 1998).

4.13. Hypocotyl length assay and seed production

For plant growth conditions see chapter 4.1. For analyzing the length of hypocotyls, 30 seeds each of Col-0, δ*oat*1, δ*oat*3, δOat-His4 and δOat-His9 were sowed on 1/5 of 14 cm Petri dishes, and grown for 14 days without light at a constant temperature of 22 °C. For analysis, seedlings were placed on a plate containing 2 % agar,

preventing the seedling from drying, photographed and computationally analysed using ImageJ (http://rsbweb.nih.gov/ij/). For analysis of the seed production *δoat* mutants and GFP-tagged δOAT overexpressing plants were grown on soil under long day (16 h light) or short day (9 h light) conditions until harvest (8-10 weeks). Total seed yield was analysed using a special accuracy scale.

4.14. Root length and leaf rosette diameter measurements

For plant growth conditions see chapter 4.1. For analyzing the root length, 4 seeds of Col-0 and δ*oat*1, respectively, were sowed in a row in the upper third of 14 cm Petri dishes (N (Petri dishes) = 25) and grown for 14 days with short day conditions at a constant temperature of 22 °C. For analysis, plates were photographed and the seedlings computationally analyzed using ImageJ (http://rsbweb.nih.gov/ij/). For analyzing root length under salt stress conditions seeds were sowed as described above on ½ MS complemented with 2 % sucrose and 50 mM NaCl. For analyzing leaf rosette diameters seeds of Col-0 and δ*oat*1, respectively, were grown on soil for 14 days. Plants without salt stress conditions were grown under standard short day conditions until first flowering (N (each line) = 20). Plants with salt stress conditions were watered with 400 ml of 50 mM NaCl twice a week until first flowering (N (each line) = 20). Leaf rosette diameters were analyzed again by the use of ImageJ.

5. References

Adams, E. and L. Frank (1980) Metabolism of proline and the hydroxyprolines. Annu Rev Biochem 49: 1005-1061

Ali, M. H. and B. Imperiali (2005) Protein oligomerization: how and why. Bioorg Med Chem 13(17): 5013-5020

Antosiewicz, D. M., D. H. Polisensky, *et al.* (1995) Cellular localization of the Ca2+ binding TCH3 protein of Arabidopsis. Plant J 8(5): 623-636

Arsova, B., S. Kierszniowska, *et al.* (2012) The use of heavy nitrogen in quantitative proteomics experiments in plants. Trends Plant Sci 17(2): 102-112

Ausubel, F. M., R. Brent, *et al.*, Eds. (1991) Current Protocols in Molecular Biology, Green Publishing Associates and Wiley-Interscience

Bagni, N. and A. Tassoni (2001) Biosynthesis, oxidation and conjugation of aliphatic polyamines in higher plants. Amino Acids 20(3): 301-317

Bahaji, A., M. Ovecka, *et al.* (2011) Dual targeting to mitochondria and plastids of AtBT1 and ZmBT1, two members of the mitochondrial carrier family. Plant Cell Physiol 52(4): 597-609

Beligni, M. V. and L. Lamattina (2000) Nitric oxide stimulates seed germination and de-etiolation, and inhibits hypocotyl elongation, three light-inducible responses in plants. Planta 210(2): 215-221

Berglund, A. K., E. Spanning, *et al.* (2009) Dual targeting to mitochondria and chloroplasts: characterization of Thr-tRNA synthetase targeting peptide. Mol Plant 2(6): 1298-1309

Bethke, P. C., F. Gubler, *et al.* (2004) Dormancy of Arabidopsis seeds and barley grains can be broken by nitric oxide. Planta 219(5): 847-855

Bewley, M. C., P. D. Jeffrey, *et al.* (1999) Crystal structures of Bacillus caldovelox arginase in complex with substrate and inhibitors reveal new insights into activation, inhibition and catalysis in the arginase superfamily. Structure 7(4): 435-448

Borrell, A., F. A. Culianez-Macia, *et al.* (1995) Arginine Decarboxylase Is Localized in Chloroplasts. Plant Physiol 109(3): 771-776

Boutin, J. P. (1982) Purification, properties and subunit structure of arginase from Iris bulbs. Eur J Biochem 127(2): 237-243

Bowsher, C. G. and A. K. Tobin (2001) Compartmentation of metabolism within mitochondria and plastids. J Exp Bot 52(356): 513-527

Brauc, S., E. De Vooght, *et al.* (2012) Overexpression of arginase in Arabidopsis thaliana influences defence responses against Botrytis cinerea. Plant Biol (Stuttg) 14 Suppl 1: 39-45

Brownfield, D. L., C. D. Todd, *et al.* (2008) Analysis of Arabidopsis arginase gene transcription patterns indicates specific biological functions for recently diverged paralogs. Plant Mol Biol 67(4): 429-440

Bruckner, A., C. Polge, *et al.* (2009) Yeast two-hybrid, a powerful tool for systems biology. Int J Mol Sci 10(6): 2763-2788

Buchanan, B. B., W. Gruissem, *et al.* (2006) Biochemistry & Molecular Biology of Plants

Bunsupa, S., K. Katayama, *et al.* (2012) Lysine decarboxylase catalyzes the first step of quinolizidine alkaloid biosynthesis and coevolved with alkaloid production in leguminosae. Plant Cell 24(3): 1202-1216

Caldovic, L. and M. Tuchman (2003) N-acetylglutamate and its changing role through evolution. Biochem J 372(Pt 2): 279-290

Cama, E., D. M. Colleluori, *et al.* (2003) Human arginase II: crystal structure and physiological role in male and female sexual arousal. Biochemistry 42(28): 8445-8451

Catoni, E., M. Desimone, *et al.* (2003) Expression pattern of a nuclear encoded mitochondrial arginine-ornithine translocator gene from Arabidopsis. BMC Plant Biol 3: 1

Chen, H., B. C. McCaig, *et al.* (2004) Regulation of plant arginase by wounding, jasmonate, and the phytotoxin coronatine. J Biol Chem 279(44): 45998-46007

Citovsky, V., L. Y. Lee*, et al.* (2006) Subcellular localization of interacting proteins by bimolecular fluorescence complementation in planta. J Mol Biol 362(5): 1120-1131

Claros, M. G. and P. Vincens (1996) Computational method to predict mitochondrially imported proteins and their targeting sequences. Eur J Biochem 241(3): 779-786

Clough, S. J. and A. F. Bent (1998) Floral dip: a simplified method for Agrobacterium-mediated transformation of Arabidopsis thaliana. Plant J 16(6): 735-743

Colleluori, D. M., R. S. Reczkowski*, et al.* (2005) Probing the role of the hyper-reactive histidine residue of arginase. Arch Biochem Biophys 444(1): 15-26

Correa-Aragunde, N., M. Graziano*, et al.* (2004) Nitric oxide plays a central role in determining lateral root development in tomato. Planta 218(6): 900-905

Crawford, N. M., M. Galli*, et al.* (2006) Plant nitric oxide synthase: back to square one - Response. Trends Plant Sci 11(11): 526-527

Cunin, R., N. Glansdorff*, et al.* (1986) Biosynthesis and metabolism of arginine in bacteria. Microbiol Rev 50(3): 314-352

Dabir, S., P. Dabir*, et al.* (2005) Purification, properties and alternate substrate specificities of arginase from two different sources: Vigna catjang cotyledon and buffalo liver. Int J Biol Sci 1(3): 114-122

Davis, R. H. (1986) Compartmental and regulatory mechanisms in the arginine pathways of Neurospora crassa and Saccharomyces cerevisiae. Microbiol Rev 50(3): 280-313

de Ruiter, H. and C. Kolloffel (1983) Arginine catabolism in the cotyledons of developing and germinating pea seeds. Plant Physiol 73(3): 525-528

Desai, H. V. (1983) Purification & properties of arginase from Arachis hypogea L. seedlings. Indian J Biochem Biophys 20(4): 236-237

Deuschle, K., D. Funck*, et al.* (2004) The role of [Delta]1-pyrroline-5-carboxylate dehydrogenase in proline degradation. Plant Cell 16(12): 3413-3425

Deuschle, K., D. Funck, *et al.* (2001) A nuclear gene encoding mitochondrial Delta-pyrroline-5-carboxylate dehydrogenase and its potential role in protection from proline toxicity. Plant J 27(4): 345-356

Di Costanzo, L., M. E. Pique, *et al.* (2007) Crystal structure of human arginase I complexed with thiosemicarbazide reveals an unusual thiocarbonyl mu-sulfide ligand in the binuclear manganese cluster. J Am Chem Soc 129(20): 6388-6389

Dougall, D. K. and M. M. Fulton (1967) Biosynthesis of protein amino acids in plant tissue culture. 3. Studies on the biosynthesis of arginine. Plant Physiol 42(3): 387-390

Dowling, D. P., L. Di Costanzo, *et al.* (2008) Evolution of the arginase fold and functional diversity. Cell Mol Life Sci 65(13): 2039-2055

Earley, K. W., J. R. Haag, *et al.* (2006) Gateway-compatible vectors for plant functional genomics and proteomics. Plant J 45(4): 616-629

Elthon, T. E. and C. R. Stewart (1981) Submitochondrial location and electron transport characteristics of enzymes involved in proline oxidation. Plant Physiol 67(4): 780-784

Elthon, T. E. and C. R. Stewart (1982) Proline Oxidation in Corn Mitochondria : Involvement of NAD, Relationship to Ornithine Metabolism, and Sidedness on the Inner Membrane. Plant Physiol 70(2): 567-572

Eurostat (2011) Agriculture and fishery statistics, Main results — 2009–10. Luxembourg, Publications Office of the European Union

Facchini, P. J., D. A. Bird, *et al.* (2004) Can Arabidopsis make complex alkaloids? Trends Plant Sci 9(3): 116-122

Fan, H. Y., Y. Hu, *et al.* (1997) Specific interactions between the K domains of AG and AGLs, members of the MADS domain family of DNA binding proteins. Plant J 12(5): 999-1010

Fischer, W. N., M. Kwart, *et al.* (1995) Substrate specificity and expression profile of amino acid transporters (AAPs) in Arabidopsis. J Biol Chem 270(27): 16315-16320

Fischer, W. N., D. D. Loo, *et al.* (2002) Low and high affinity amino acid H+-cotransporters for cellular import of neutral and charged amino acids. Plant J 29(6): 717-731

Flores, T., C. D. Todd, *et al.* (2008) Arginase-negative mutants of Arabidopsis exhibit increased nitric oxide signaling in root development. Plant Physiol 147(4): 1936-1946

Foresi, N., N. Correa-Aragunde, *et al.* (2010) Characterization of a nitric oxide synthase from the plant kingdom: NO generation from the green alga Ostreococcus tauri is light irradiance and growth phase dependent. Plant Cell 22(11): 3816-3830

Forsum, O., H. Svennerstam, *et al.* (2008) Capacities and constraints of amino acid utilization in Arabidopsis. New Phytol 179(4): 1058-1069

Funck, D. (2001). Glucose and proline dependent signal transduction in Arabidopsis : contributions to balancing life and death**:** VIII, 89 S.

Funck, D., S. Eckard, *et al.* (2010) Non-redundant functions of two proline dehydrogenase isoforms in Arabidopsis. BMC Plant Biol 10: 70

Funck, D., B. Stadelhofer, *et al.* (2008) Ornithine-delta-aminotransferase is essential for arginine catabolism but not for proline biosynthesis. BMC Plant Biol 8: 40

Funck, D., G. Winter, *et al.* (2012) Requirement of proline synthesis during Arabidopsis reproductive development. BMC Plant Biol 12: 191

Gietz, R. D. and R. A. Woods (2002) Transformation of yeast by lithium acetate/single-stranded carrier DNA/polyethylene glycol method. Guide to Yeast Genetics and Molecular and Cell Biology, Pt B 350: 87-96

Goldraij, A. and J. C. Polacco (2000) Arginine degradation by arginase in mitochondria of soybean seedling cotyledons. Planta 210(4): 652-658

Goodsell, D. S. (1991) Inside a living cell. Trends Biochem Sci 16(6): 203-206

Goodsell, D. S. and A. J. Olson (1993) Soluble proteins: size, shape and function. Trends Biochem Sci 18(3): 65-68

Goodsell, D. S. and A. J. Olson (2000) Structural symmetry and protein function. Annu Rev Biophys Biomol Struct 29: 105-153

Gupta, K. J., A. R. Fernie*, et al.* (2011) On the origins of nitric oxide. Trends Plant Sci 16(3): 160-168

Haferkamp, I. and S. Schmitz-Esser (2012) The plant mitochondrial carrier family: functional and evolutionary aspects. Front Plant Sci 3: 2

Hajdukiewicz, P., Z. Svab*, et al.* (1994) The small, versatile pPZP family of Agrobacterium binary vectors for plant transformation. Plant Mol Biol 25(6): 989-994

Hanfrey, C., S. Sommer*, et al.* (2001) Arabidopsis polyamine biosynthesis: absence of ornithine decarboxylase and the mechanism of arginine decarboxylase activity. Plant J 27(6): 551-560

Hanzawa, Y., A. Imai*, et al.* (2002) Characterization of the spermidine synthase-related gene family in Arabidopsis thaliana. FEBS Lett 527(1-3): 176-180

Hodges, M. (2002) Enzyme redundancy and the importance of 2-oxoglutarate in plant ammonium assimilation. J Exp Bot 53(370): 905-916

Hong, Z., K. Lakkineni*, et al.* (2000) Removal of feedback inhibition of delta(1)-pyrroline-5-carboxylate synthetase results in increased proline accumulation and protection of plants from osmotic stress. Plant Physiol 122(4): 1129-1136

Hoyos, M. E., L. Palmieri*, et al.* (2003) Identification of a mitochondrial transporter for basic amino acids in Arabidopsis thaliana by functional reconstitution into liposomes and complementation in yeast. Plant J 33(6): 1027-1035

Hwang, H. J., E. H. Kim*, et al.* (2001) Isolation and properties of arginase from a shade plant, ginseng (Panax ginseng C.A. Meyer) roots. Phytochemistry 58(7): 1015-1024

Illingworth, C., M. J. Mayer*, et al.* (2003) The diverse bacterial origins of the Arabidopsis polyamine biosynthetic pathway. FEBS Lett 549(1-3): 26-30

Janowitz, T., H. Kneifel*, et al.* (2003) Identification and characterization of plant agmatine iminohydrolase, the last missing link in polyamine biosynthesis of plants. FEBS Lett 544(1-3): 258-261

Jones, S. and J. M. Thornton (1996) Principles of protein-protein interactions. Proc Natl Acad Sci U S A 93(1): 13-20

Kang, J. H. and Y. D. Cho (1990) Purification and Properties of Arginase from Soybean, Glycine max, Axes. Plant Physiol 93(3): 1230-1234

Kanyo, Z. F., L. R. Scolnick, *et al.* (1996) Structure of a unique binuclear manganese cluster in arginase. Nature 383(6600): 554-557

Kaundal, R., R. Saini, *et al.* (2010) Combining machine learning and homology-based approaches to accurately predict subcellular localization in Arabidopsis. Plant Physiol 154(1): 36-54

Kavi Kishor, P. B. and N. Sreenivasulu (2013) Is proline accumulation per se correlated with stress tolerance or is proline homoeostasis a more critical issue? Plant Cell Environ

Kelley, L. A. and M. J. E. Sternberg (2009) Protein structure prediction on the Web: a case study using the Phyre server. Nature Protocols 4(3): 363-371

King, J. E. and D. J. Gifford (1997) Amino Acid Utilization in Seeds of Loblolly Pine during Germination and Early Seedling Growth (I. Arginine and Arginase Activity). Plant Physiol 113(4): 1125-1135

Krouk, G., N. M. Crawford, *et al.* (2010) Nitrate signaling: adaptation to fluctuating environments. Curr Opin Plant Biol 13(3): 266-273

Krumpelman, P. M., S. K. Freyermuth, *et al.* (1995) Nucleotide sequence of Arabidopsis thaliana arginase expressed in yeast. Plant Physiol 107(4): 1479-1480

Kupper, H., I. Setlik, *et al.* (2008) Iron limitation in the marine cyanobacterium Trichodesmium reveals new insights into regulation of photosynthesis and nitrogen fixation. New Phytol 179(3): 784-798

Laemmli, U. K. (1970) Cleavage of structural proteins during the assembly of the head of bacteriophage T4. Nature 227(5259): 680-685

Lawand, S., A. J. Dorne, *et al.* (2002) Arabidopsis A BOUT DE SOUFFLE, which is homologous with mammalian carnitine acyl carrier, is required for postembryonic growth in the light. Plant Cell 14(9): 2161-2173

Llacer, J. L., I. Fita*, et al.* (2008) Arginine and nitrogen storage. Curr Opin Struct Biol

Lunn, J. E. (2007) Compartmentation in plant metabolism. J Exp Bot 58(1): 35-47

Martin-Falquina, A. and M. E. Legaz (1984) Purification and Properties of the Constitutive Arginase of Evernia prunastri. Plant Physiol 76(4): 1065-1069

Masclaux-Daubresse, C., M. Reisdorf-Cren*, et al.* (2006) Glutamine synthetase-glutamate synthase pathway and glutamate dehydrogenase play distinct roles in the sink-source nitrogen cycle in tobacco. Plant Physiol 140(2): 444-456

Mathews, C. K. (1993) The cell-bag of enzymes or network of channels? J Bacteriol 175(20): 6377-6381

Micallef, B. J. and B. J. Shelp (1989) Arginine metabolism in developing soybean cotyledons : I. Relationship to nitrogen nutrition. Plant Physiol 90(2): 624-630

Miller, G., A. Honig*, et al.* (2009) Unraveling delta1-pyrroline-5-carboxylate-proline cycle in plants by uncoupled expression of proline oxidation enzymes. J Biol Chem 284(39): 26482-26492

Morris, C. J., J. F. Thompson*, et al.* (1969) Metabolism of Glutamic Acid and N-Acetylglutamic Acid in Leaf Discs and Cell-free Extracts of Higher Plants. Plant Physiol 44(7): 1023-1026

Murashige, T. and F. Skoog (1962) A Revised Medium for Rapid Growth and Bio Assays with Tobacco Tissue Cultures. Physiologia Plantarum 15(3): 473-497

Murcha, M. W., D. Elhafez*, et al.* (2007) Characterization of the preprotein and amino acid transporter gene family in Arabidopsis. Plant Physiol 143(1): 199-212

Nakagawa, T., T. Kurose*, et al.* (2007) Development of series of gateway binary vectors, pGWBs, for realizing efficient construction of fusion genes for plant transformation. J Biosci Bioeng 104(1): 34-41

Neill, S., R. Barros*, et al.* (2008) Nitric oxide, stomatal closure, and abiotic stress. J Exp Bot 59(2): 165-176

Niyogi, K. K., R. L. Last, *et al.* (1993) Suppressors of trp1 fluorescence identify a new arabidopsis gene, TRP4, encoding the anthranilate synthase beta subunit. Plant Cell 5(9): 1011-1027

Okumoto, S., W. Koch, *et al.* (2004) Root phloem-specific expression of the plasma membrane amino acid proton co-transporter AAP3. J Exp Bot 55(406): 2155-2168

Ovadi, J. and P. A. Srere (2000) Macromolecular compartmentation and channeling. Int Rev Cytol 192: 255-280

Palmieri, L., V. De Marco, *et al.* (1997) Identification of the yeast ARG-11 gene as a mitochondrial ornithine carrier involved in arginine biosynthesis. FEBS Lett 410(2-3): 447-451

Palmieri, L., C. D. Todd, *et al.* (2006) Arabidopsis mitochondria have two basic amino acid transporters with partially overlapping specificities and differential expression in seedling development. Biochim Biophys Acta 1757(9-10): 1277-1283

Phang, J. M. (1985) The regulatory functions of proline and pyrroline-5-carboxylic acid. Curr Top Cell Regul 25: 91-132

Picault, N., M. Hodges, *et al.* (2004) The growing family of mitochondrial carriers in Arabidopsis. Trends Plant Sci 9(3): 138-146

Piotrowski, M., T. Janowitz, *et al.* (2003) Plant C-N hydrolases and the identification of a plant N-carbamoylputrescine amidohydrolase involved in polyamine biosynthesis. J Biol Chem 278(3): 1708-1712

Pudelski, B., S. Kraus, *et al.* (2010) The plant PRAT proteins - preprotein and amino acid transport in mitochondria and chloroplasts. Plant Biol (Stuttg) 12 Suppl 1: 42-55

Qiao, W. and L. M. Fan (2008) Nitric oxide signaling in plant responses to abiotic stresses. J Integr Plant Biol 50(10): 1238-1246

Radwanski, E. R. and R. L. Last (1995) Tryptophan biosynthesis and metabolism: biochemical and molecular genetics. Plant Cell 7(7): 921-934

Roosens, N. H., F. A. Bitar, *et al.* (2002) Overexpression of ornithine-d-aminotransferase increases proline biosynthesis and confers osmotolerance in transgenic plants. Molecular Breeding 9(2): 73-80

Roosens, N. H., T. T. Thu, *et al.* (1998) Isolation of the ornithine-delta-aminotransferase cDNA and effect of salt stress on its expression in Arabidopsis thaliana. Plant Physiol 117(1): 263-271

Sabio, G., A. Mora, *et al.* (2001) Glu-256 is a main structural determinant for oligomerisation of human arginase I. FEBS Lett 501(2-3): 161-165

Sambrook, J., E. F. Fritsch, *et al.* (1989) Molecular Cloning. Cold Spring Habor, NY, Cold Spring Harbor Laboratory Press

Schonichen, A., B. A. Webb, *et al.* (2013) Considering protonation as a posttranslational modification regulating protein structure and function. Annu Rev Biophys 42: 289-314

Schuhmann, H., U. Mogg, *et al.* (2011) A new principle of oligomerization of plant DEG7 protease based on interactions of degenerated protease domains. Biochem J 435(1): 167-174

Shargool, P. D., J. C. Jain, *et al.* (1988) Ornithine Biosynthesis, and Arginine-Biosynthesis and Degradation in Plant-Cells. Phytochemistry 27(6): 1571-1574

Shi, H., T. Ye, *et al.* (2013) Manipulation of arginase expression modulates abiotic stress tolerance in Arabidopsis: effect on arginine metabolism and ROS accumulation. J Exp Bot

Slocum, R. D. (2005) Genes, enzymes and regulation of arginine biosynthesis in plants. Plant Physiology and Biochemistry 43(8): 729-745

Spivey, H. O. and J. Ovadi (1999) Substrate channeling. Methods 19(2): 306-321

Srere, P. A. (2000) Macromolecular interactions: tracing the roots. Trends Biochem Sci 25(3): 150-153

Stellberger, T., R. Hauser, *et al.* (2010) Improving the yeast two-hybrid system with permutated fusions proteins: the Varicella Zoster Virus interactome. Proteome Sci 8: 8

Stranska, J., D. Kopecny, *et al.* (2008) Ornithine delta-aminotransferase: An enzyme implicated in salt tolerance in higher plants. Plant Signal Behav 3(11): 929-935

Stranska, J., M. Tylichova, *et al.* (2010) Biochemical characterization of pea ornithine-delta-aminotransferase: substrate specificity and inhibition by di- and polyamines. Biochimie 92(8): 940-948

Svennerstam, H., U. Ganeteg, *et al.* (2008) Root uptake of cationic amino acids by Arabidopsis depends on functional expression of amino acid permease 5. New Phytol

Thompson, J. D., D. G. Higgins, *et al.* (1994) CLUSTAL W: improving the sensitivity of progressive multiple sequence alignment through sequence weighting, position-specific gap penalties and weight matrix choice. Nucleic Acids Res 22(22): 4673-4680

Todd, C. D., J. E. Cooke, *et al.* (2001) Regulation of loblolly pine (Pinus taeda L.) arginase in developing seedling tissue during germination and post-germinative growth. Plant Mol Biol 45(5): 555-565

Todd, C. D. and D. J. Gifford (2002) The role of the megagametophyte in maintaining loblolly pine (Pinus taeda L.) seedling arginase gene expression in vitro. Planta 215(1): 110-118

Toka, I., S. Planchais, *et al.* (2010) Mutations in the hyperosmotic stress-responsive mitochondrial BASIC AMINO ACID CARRIER2 enhance proline accumulation in Arabidopsis. Plant Physiol 152(4): 1851-1862

Towbin, H., T. Staehelin, *et al.* (1979) Electrophoretic transfer of proteins from polyacrylamide gels to nitrocellulose sheets: procedure and some applications. Proc Natl Acad Sci U S A 76(9): 4350-4354

Tun, N. N., C. Santa-Catarina, *et al.* (2006) Polyamines induce rapid biosynthesis of nitric oxide (NO) in Arabidopsis thaliana seedlings. Plant Cell Physiol 47(3): 346-354

VanEtten, C. H., R. W. Miller, *et al.* (1963) Amino Acid Composition of Seeds from 200 Angiospermous Plant Species. Agricultural and Food Chemistry 11(5): 399-410

Verslues, P. E. and R. E. Sharp (1999) Proline accumulation in maize (Zea mays L.) primary roots at low water potentials. II. Metabolic source of increased proline deposition in the elongation zone. Plant Physiol 119(4): 1349-1360

Vogel, H. J. and D. M. Bonner (1956) Acetylornithinase of Escherichia coli: partial purification and some properties. J Biol Chem 218(1): 97-106

Walden, H., G. S. Bell, *et al.* (2001) Tiny TIM: a small, tetrameric, hyperthermostable triosephosphate isomerase. J Mol Biol 306(4): 745-757

Williams, I. and L. Frank (1975) Improved chemical synthesis and enzymatic assay of delta-1-pyrroline-5-carboxylic acid. Anal Biochem 64(1): 85-97

Winkel, B. S. (2004) Metabolic channeling in plants. Annu Rev Plant Biol 55: 85-107

Witte, C. P. (2011) Urea metabolism in plants. Plant Sci 180(3): 431-438

Yamada, K., J. Lim, *et al.* (2003) Empirical analysis of transcriptional activity in the Arabidopsis genome. Science 302(5646): 842-846

Yamasaki, H. and M. F. Cohen (2006) NO signal at the crossroads: polyamine-induced nitric oxide synthesis in plants? Trends Plant Sci 11(11): 522-524

Yuan, L., D. Loque, *et al.* (2007) The organization of high-affinity ammonium uptake in Arabidopsis roots depends on the spatial arrangement and biochemical properties of AMT1-type transporters. Plant Cell 19(8): 2636-2652

Zonia, L. E., N. E. Stebbins, *et al.* (1995) Essential role of urease in germination of nitrogen-limited Arabidopsis thaliana seeds. Plant Physiol 107(4): 1097-1103

6. Acknowledgements

I would like to thank Prof. Dr. Iwona Adamska for the opportunity to carry out this research project in her lab as well as for her professional mentoring, encouragement and the freedom of work.

I am especially grateful to Dr. Dietmar Funck for teaching me all of Arabidopsis research, enduring all of my questions and leading me to many ideas regarding this work. I profited a lot from Dietmar's tremendous preparatory work and his tireless willingness for discussion and cooperation.

I also like to thank Prof. Dr. Elisa May to act as referee and examiner for this thesis as well as her group, the Bioimaging Centre of the University of Konstanz, especially Daniela Hermann, for the tireless help with the LSM and digital imaging.

Additional thanks to Prof. Dr. Doris Rentsch to act as the third examiner.

My thanks also to Dr. Holger Schuhmann for teaching me the basics and subtleties of Y2H and Dr. Jens Lohscheider for all the subtleties in protein detection as well as structure modeling. Additional thanks to Luise Schönemann for communicating results prior to publication.

I would like to thank Silvia Kuhn, Rowitha Miller, Regina Grimm, Ulrike Mogg and Manuela Perthold as well as all the other members of the Adamska group for the pleasant working atmosphere, for helpful advice and for all the delicious cakes and barbeques.

Many thanks to Michaela Böhne, representative for the whole team of gardeners, who excellently nourished all my Arabidopsis plants.

I am very grateful to Helgard Fischer, Dr. Dietmar Funck and Dr. Jens Lohscheider taking care of my written English and critical revision of this thesis.

I would like to thank the Stiftung der deutschen Wirtschaft (sdw) who paid for my living by a grant.

My most sincere thanks to Peter Winter for his permanent support in all areas of our shared lifes.